

Selection Rules of a simple model of a  
Quantum Dot

University of Copenhagen

Buyuan Luo

Supervisor: Anders Søndberg Sørensen

30/11/2021

# Acknowledgements

I want to thank my parents for their long time support. I want to thank my supervisor Anders for his patient and careful guidance. I want to thank my friend Xiangyu Lin for helping me with coding and plotting.

# Contents

<b>1</b>	<b>Introduction</b>	<b>3</b>
<b>2</b>	<b>Review of Hydrogen Atom</b>	<b>4</b>
2.1	States . . . . .	4
2.1.1	Fine structure . . . . .	5
2.1.2	Weak Zeeman Effect . . . . .	5
2.1.3	Case $\vec{B} \parallel \vec{z}$ . . . . .	7
2.1.4	Case $\vec{B} \perp \vec{z}$ . . . . .	7
2.2	Selection Rules . . . . .	10
2.2.1	Matrix element of electric dipole transitions . . . . .	10
2.2.2	selection rules with $\vec{B} \parallel \vec{z}$ . . . . .	10
2.2.3	selection rules with $\vec{B} \perp \vec{z}$ . . . . .	12
<b>3</b>	<b>Quantum Dots</b>	<b>13</b>
3.1	A simple model of a quantum dot . . . . .	13
3.1.1	band structure . . . . .	13
3.1.2	Carrier configuration . . . . .	14
3.1.3	states of a quantum dot . . . . .	14
3.1.4	bands splitting $\Delta_{lh-hh}$ . . . . .	15
3.2	Selection Rules . . . . .	16
3.2.1	Interband transitions . . . . .	16
3.2.2	adding $\vec{B} \parallel \vec{z}$ . . . . .	17
3.2.3	adding $\vec{B} \perp \vec{z}$ . . . . .	17
<b>4</b>	<b>Regimes with <math>\beta</math></b>	<b>19</b>
4.1	Effect of Strain anistropy $\beta$ . . . . .	19
4.2	Regime $\Delta \gg \beta$ . . . . .	20
4.3	limit $\beta \gg \Delta$ . . . . .	24
4.4	overall regime . . . . .	26
<b>5</b>	<b>Conclusion and Outlook</b>	<b>38</b>

# Chapter 1

## Introduction

Quantum dots are nano-scale semiconductor particles showing optical properties predicted by quantum mechanics. As 'artificial atoms', Qdots have energy spectrum with discrete energy levels and can be measured and manipulated by light. Physics of spin and angular momentum in Qdots are what intriguing to research. By exploiting the physics of Qdots, people may store qubit in the QD, a very nice two level system. It is clear that qubit are basis of quantum computation and quantum information processing. In short, QDs are potential nano-structural device with broad application prospects in the field of quantum information. There are several technicals (through epitaxial or chemical growth) to make a quantum dot nowadays, but in the present work, we only focus on physics in Stranski-Krastanov quantum dots, especially, the CdSe/ZnSe QD. We are motivated by the article[6]. Specifically, In this thesis, we focus on coupling of a single quantum dot with electromagnetic fields.

In general, QDs exhibit different selection rules from real atom (for instance the hydrogen atom) due to QDs' specific structure and symmetry. We want to theoretically model a simple quantum dot and see how its dipole transitions are controlled by the strain effect. In this thesis, we first review selection rules for fine structure of hydrogen atom under an external magnetic field, then for a single particle QD[2]. In the case of QD, we will see photons emitted by QD are linearly polarised and highly dependent on rotation of an external transverse magnetic field until we consider attribution of strain anisotropy effect.

# Chapter 2

## Review of Hydrogen Atom

Before we start study of selection rules for a quantum dot, we review that for a hydrogen atom and some basic quantum mechanics from books [4][3]. Generally, in this chapter, we first review the states of fine structure of a hydrogen atom, then we consider weak Zeeman effect as a small perturbation, and derive new states. Finally, we calculate electric dipole transitions among these states. As an important result, we will also see how the polarisations of emitted photon due to electric dipole transition are highly dependent on rotation of external magnetic field.

### 2.1 States

Under spherical coordinate, the spatial wave function of an electron in hydrogen atom can be written as product of radial function  $R(r)$  and spherical harmonics  $Y(\theta, \phi)$  labeled by principle quantum number  $n$ , Azimuthal quantum number  $l$  and magnetic quantum number  $m_l$ .

$$\psi_{nlm}(r, \theta, \phi) = R_{nl}(r)Y_l^m(\theta, \phi)$$

where states with same quantum number  $n$  are degenerate.  $l$  and  $m_l$  are physical quantities about angular momentum. Note that relation of these three quantum numbers are given:  $n = 0, 1, 2, 3, \dots$ ;  $l = 0, 1, 2, \dots, n - 1$ ;  $m_l = -l, -l + 1, \dots, l - 1, l + 1$

As we always want to consider transitions of two-level system, in this case, we need wave functions for ground states ( $n = 1$ ) and first excited states ( $n = 2$ ):

$$\psi_{100}(r, \theta, \phi) = \frac{1}{\sqrt{\pi a^3/2}} e^{-r/a}$$
$$\psi_{200}(r, \theta, \phi) = \frac{\sqrt{2}}{8\sqrt{\pi a^5/2}} r e^{-r/(2a)} \cos(\theta)$$

$$\psi_{21\pm 1}(r, \theta, \phi) = \mp \frac{1}{8\sqrt{\pi}a^{5/2}} r e^{-r/(2a)} \sin(\theta) e^{\pm i\phi}$$

where  $a$  is the Bohr radius. Certainly, these wave functions are mutually orthogonal.

### 2.1.1 Fine structure

A more realistic model for hydrogen is made by adding small corrections due to relativistic correction and spin-orbit coupling. The total Hamiltonian of the system is given by:

$$H_{tot} = -\frac{\hbar^2}{2m} \nabla^2 - \frac{e^2}{4\pi\epsilon_0} \frac{1}{r} - \frac{p^4}{8m^3c^2} + \left( \frac{e^2}{8\pi\epsilon_0} \right) \frac{1}{m^2c^2r^3} \vec{S} \cdot \vec{L}$$

where on the right the first two terms are interaction of the electron with nucleus through Coulomb force, the third and fourth terms are respectively relativistic correction and spin-orbital interaction. By treating two corrections as small perturbations, we can use non-degenerate perturbation theory to calculate first order energy correction. So we have energy levels for the total Hamiltonian given by:

$$E = -\frac{13.6eV}{n^2} \left[ 1 + \frac{\alpha^2}{n^2} \left( \frac{n}{j+1/2} - \frac{3}{4} \right) \right]$$

where  $\alpha$  is fine structure constant. From this equation we see that the degeneracy of the states depends on not only principle quantum number  $n$  but also total angular momentum  $j$ . We also note that both spin and orbital angular momenta do not commute with the Hamiltonian of spin-orbital interactions. So  $n, l, m_l$  are no longer good quantum numbers to label states of the new system, instead we use  $n, l, j, m_j$ . Note that  $j = l \pm 1/2$  when  $l \neq 0$ , and  $j = 1/2$  when  $l = 0$ .

### 2.1.2 Weak Zeeman Effect

Zeeman effect is a phenomenon that when an external magnetic field is placed on an atom, energy levels of electron are shifted due to spin-orbital coupling. The Hamiltonian of this effect is given:

$$H'_{zm} = \frac{e}{2m_e c} \left( \vec{L} + g_e \vec{S} \right) \cdot \vec{B} \quad (2.1)$$

where  $g_e$  is the electron spin  $g$  factor, for simplicity of calculation, we let it equals to 2. In this part we only consider the case where Zeeman effect is

much small compared to fine structure corrections. That is, we will treat the Hamiltonian of Zeeman effect as small perturbation and let the fine structure term as unperturbed.

Now we express the states characterized by  $l, j, m_j$  into liner combination of  $|lm_l\rangle |sm_s\rangle$  using the Clebsch-Gorden coefficients. Review that:

C-G Coefficients	$m_s = 1/2$	$m_s = -1/2$
$j = l + 1/2$	$\sqrt{\frac{l + m_j + 1/2}{2l + 1}}$	$\sqrt{\frac{l - m_j + 1/2}{2l + 1}}$
$j = l - 1/2$	$-\sqrt{\frac{l - m_j + 1/2}{2l + 1}}$	$\sqrt{\frac{l + m_j + 1/2}{2l + 1}}$

Also by only considering ground state  $n=1$  and first excited state  $n=2$ , we have quantum numbers  $n = 1, 2$ ;  $l=0,1$ ;  $j = \frac{1}{2}, \frac{3}{2}$ ;  $m_j = \pm\frac{1}{2}, \pm\frac{3}{2}$ . And write down all possible states and label them with numbers for the sake of convenience: **Ms**

$$|nljm_j\rangle = \sum |lm_l\rangle |sm_s\rangle = |number\rangle.$$

Ground states:

$$|10\frac{1}{2}\frac{1}{2}\rangle = |00\rangle |\frac{1}{2}\frac{1}{2}\rangle \equiv |7\rangle$$

$$|10\frac{1}{2}\frac{-1}{2}\rangle = |00\rangle |\frac{1}{2}\frac{-1}{2}\rangle \equiv |8\rangle$$

First excited states:

$$l = 0, j = 1/2$$

$$|20\frac{1}{2}\frac{1}{2}\rangle = |00\rangle |\frac{1}{2}\frac{1}{2}\rangle \equiv |9\rangle$$

$$|20\frac{1}{2}\frac{-1}{2}\rangle = |00\rangle |\frac{1}{2}\frac{-1}{2}\rangle \equiv |10\rangle$$

$$l = 1, j = 3/2$$

$$|21\frac{3}{2}\frac{3}{2}\rangle = |11\rangle |\frac{1}{2}\frac{-1}{2}\rangle \equiv |1\rangle$$

$$|21\frac{3}{2}\frac{1}{2}\rangle = \sqrt{\frac{2}{3}} |10\rangle |\frac{1}{2}\frac{1}{2}\rangle + \sqrt{\frac{1}{3}} |11\rangle |\frac{1}{2}\frac{-1}{2}\rangle \equiv |2\rangle$$

$$|21\frac{3}{2}\frac{-1}{2}\rangle = \sqrt{\frac{1}{3}} |1-1\rangle |\frac{1}{2}\frac{1}{2}\rangle + \sqrt{\frac{2}{3}} |10\rangle |\frac{1}{2}\frac{-1}{2}\rangle \equiv |3\rangle$$

$$|21\frac{3}{2}\frac{-3}{2}\rangle = |1-1\rangle |\frac{1}{2}\frac{-1}{2}\rangle \equiv |4\rangle$$

$$l = 1, j = 1/2$$

$$|21\frac{1}{2}\frac{1}{2}\rangle = -\sqrt{\frac{1}{3}} |10\rangle |\frac{1}{2}\frac{1}{2}\rangle + \sqrt{\frac{2}{3}} |11\rangle |\frac{1}{2}\frac{-1}{2}\rangle \equiv |5\rangle$$

$$|21\frac{1}{2}\frac{-1}{2}\rangle = -\sqrt{\frac{2}{3}} |1-1\rangle |\frac{1}{2}\frac{1}{2}\rangle + \sqrt{\frac{1}{3}} |10\rangle |\frac{1}{2}\frac{-1}{2}\rangle \equiv |6\rangle$$

In the case without an external magnetic field, states above with same  $n, l, j$  are degenerate. With the external  $\vec{B}$ , these states split into two with different energy due to direction of spin.

### 2.1.3 Case $\vec{B} \parallel \vec{z}$

In case an external magnetic field parallel to z direction is placed on the atom, the Hamiltonian becomes:

$$\vec{H}_{zm} = \frac{e}{2m_e c} B_0 (L_z + 2S_z) \quad (2.2)$$

The way to get the matrix form of this Hamiltonian is by calculating matrix elements using  $\langle i | H_z | j \rangle$ , and choose the degenerate states in previous subsection as groups of basis. Also it is noted that these basis states are also eigenbasis of  $L_z$  and  $S_z$ , so the Hamiltonian is already diagonal as shown below.

For states with  $l = 0, j = 1/2$ :

$$H'_{zm} = \begin{pmatrix} 1 & 0 \\ 0 & -1 \end{pmatrix} \mu_B B_0$$

This Hamiltonian has basis either states  $|7\rangle, |8\rangle$  or  $|9\rangle, |10\rangle$

For states with  $l = 1, j = 1/2$  (basis states  $|5\rangle, |6\rangle$ ):

$$H'_{zm} = \begin{pmatrix} 1/3 & 0 \\ 0 & -1/3 \end{pmatrix} \mu_B B_0$$

For states with  $l = 1, j = 3/2$  (basis states  $|1\rangle, |2\rangle, |3\rangle, |4\rangle$ ):

$$H'_{zm} = \begin{pmatrix} 2 & 0 & 0 & 0 \\ 0 & 2/3 & 0 & 0 \\ 0 & 0 & -2/3 & 0 \\ 0 & 0 & 0 & -2 \end{pmatrix} \mu_B B_0$$

where  $\mu_B \equiv e\hbar/(2m_e c)$  is the Bohr magneton. All three Hamiltonian above are diagonal therefore these states are still good basis for the whole system. This implies that electric dipole transitions in this case is also same as the situation without the magnetic field, which we talk about in later section.

### 2.1.4 Case $\vec{B} \perp \vec{z}$

Now in case the external magnetic field is perpendicular to  $\hat{z}$ -axis, which is to say, it is parallel to  $\hat{x}\hat{y}$  plane.

$$\vec{B} = B_0(\cos\theta\vec{x} + \sin\theta\vec{y})$$

Insert it into the Eq 2.1, the Hamiltonian becomes:

$$H_{zm} = MB_0 [\cos\theta L_x + \sin\theta L_y + 2(\cos\theta S_x + \sin\theta S_y)] \quad (2.3)$$

where  $M \equiv e/(2m_e c)$ . Now review that operators  $L_x, L_y, S_x$  and  $S_y$  can be decomposed into combination of raising and lowering operators:

$$L_x = 1/2(L_+ + L_-) \text{ and } L_y = -i/2(L_+ - L_-)$$

$$S_x = 1/2(S_+ + S_-) \text{ and } S_y = -i/2(S_+ - S_-)$$

then Eq 2.3 can be rewritten in terms of raising and lowering operators:

$$H_{zm} = MB_0 [1/2(e^{-i\theta}L_+ + e^{i\theta}L_-) + e^{-i\theta}S_+ + e^{i\theta}S_-] \quad (2.4)$$

Here before calculating the matrix elements  $\langle i | H_z | j \rangle$  we review that:

$$L_+ Y_l^m = \hbar \sqrt{(l-m)(l+m+1)} Y_l^{m+1}$$

$$L_- Y_l^m = \hbar \sqrt{(l+m)(l-m+1)} Y_l^{m-1}$$

$$S_{\pm} |sm\rangle = \hbar \sqrt{s(s+1) - m(m \pm 1)} |s(m \pm 1)\rangle$$

Then the matrix form of Eq 2.3 can be calculated using states in Sec 2.1.2 as basis:

For states with  $l = 0, j = 1/2$ :

$$H_{zm} = \mu_B B_0 \begin{pmatrix} 0 & e^{-i\theta} \\ e^{i\theta} & 0 \end{pmatrix} \quad (2.5)$$

For states with  $l = 1, j = 1/2$ :

$$H_{zm} = \mu_B B_0 \begin{pmatrix} 0 & \frac{1}{3}e^{-i\theta} \\ \frac{1}{3}e^{i\theta} & 0 \end{pmatrix} \quad (2.6)$$

For states with  $l = 1, j = 3/2$ :

$$H_{zm} = \mu_B B_0 \begin{pmatrix} 0 & \frac{2}{3}\sqrt{3}e^{-i\theta} & 0 & 0 \\ \frac{2}{3}\sqrt{3}e^{-i\theta} & 0 & \frac{4}{3}e^{-i\theta} & 0 \\ 0 & \frac{4}{3}e^{i\theta} & 0 & \frac{2}{3}\sqrt{3}e^{-i\theta} \\ 0 & 0 & \frac{2}{3}\sqrt{3}e^{i\theta} & 0 \end{pmatrix} \quad (2.7)$$

Since these Hamiltonian are not diagonal, the basis states in Sec 2.1.2 are not their eigenstates. But their eigenstates can be formed as linear combination of these states according to degenerate perturbation theory. Then the next step is to diagonalize these three matrices, and using their eigenvectors as coefficients of the linear combination, then we find out the new appropriate states for the whole system.

For both Matrix(2.5) and Matrix(2.6), eigenvectors are:

$$\begin{bmatrix} 1 \\ e^{-\frac{1}{2}i\theta} \end{bmatrix}, \begin{bmatrix} -1 \\ e^{\frac{1}{2}i\theta} \end{bmatrix} \quad (2.8)$$

New states are:

$$\begin{cases} |5\rangle_{new} = e^{-\frac{1}{2}i\theta} |5\rangle + e^{\frac{1}{2}i\theta} |6\rangle \\ |6\rangle_{new} = -e^{-\frac{1}{2}i\theta} |5\rangle + e^{\frac{1}{2}i\theta} |6\rangle \end{cases} \quad (2.9)$$

$$\begin{cases} |7\rangle_{new} = e^{-\frac{1}{2}i\theta} |7\rangle + e^{\frac{1}{2}i\theta} |8\rangle \\ |8\rangle_{new} = -e^{-\frac{1}{2}i\theta} |7\rangle + e^{\frac{1}{2}i\theta} |8\rangle \end{cases} \quad (2.10)$$

$$\begin{cases} |9\rangle_{new} = e^{-\frac{1}{2}i\theta} |9\rangle + e^{\frac{1}{2}i\theta} |10\rangle \\ |10\rangle_{new} = -e^{-\frac{1}{2}i\theta} |9\rangle + e^{\frac{1}{2}i\theta} |10\rangle \end{cases} \quad (2.11)$$

For Matrix(2.7), eigenvectors are:

$$\begin{bmatrix} 3 \\ e^{-\frac{3}{2}i\theta} \\ \sqrt{3}e^{-\frac{1}{2}i\theta} \\ \sqrt{3}e^{\frac{1}{2}i\theta} \\ 3 \\ e^{\frac{3}{2}i\theta} \end{bmatrix}, \begin{bmatrix} -3 \\ -e^{-\frac{3}{2}i\theta} \\ \sqrt{3}e^{-\frac{1}{2}i\theta} \\ -\sqrt{3}e^{\frac{1}{2}i\theta} \\ 3 \\ e^{\frac{3}{2}i\theta} \end{bmatrix}, \begin{bmatrix} -\frac{3}{2} \\ -e^{-\frac{3}{2}i\theta} \\ -\frac{1}{\sqrt{3}}e^{-\frac{1}{2}i\theta} \\ \frac{1}{\sqrt{3}}e^{\frac{1}{2}i\theta} \\ 3 \\ e^{\frac{3}{2}i\theta} \end{bmatrix}, \begin{bmatrix} \frac{3}{2} \\ e^{-\frac{3}{2}i\theta} \\ -\frac{1}{\sqrt{3}}e^{-\frac{1}{2}i\theta} \\ -\frac{1}{\sqrt{3}}e^{\frac{1}{2}i\theta} \\ 3 \\ e^{\frac{3}{2}i\theta} \end{bmatrix} \quad (2.12)$$

Corresponding new states are:

$$\begin{cases} |1\rangle_{new} = \frac{1}{2\sqrt{2}}(e^{-\frac{3}{2}i\theta} |1\rangle + \sqrt{3}e^{-\frac{1}{2}i\theta} |2\rangle + \sqrt{3}e^{\frac{1}{2}i\theta} |3\rangle + e^{\frac{3}{2}i\theta} |4\rangle) \\ |2\rangle_{new} = \frac{1}{2\sqrt{2}}(-e^{-\frac{3}{2}i\theta} |1\rangle + \sqrt{3}e^{-\frac{1}{2}i\theta} |2\rangle - \sqrt{3}e^{\frac{1}{2}i\theta} |3\rangle + e^{\frac{3}{2}i\theta} |4\rangle) \\ |3\rangle_{new} = \frac{1}{2\sqrt{2}}(-e^{-\frac{3}{2}i\theta} |1\rangle - \frac{1}{\sqrt{3}}e^{-\frac{1}{2}i\theta} |2\rangle + \frac{1}{\sqrt{3}}e^{\frac{1}{2}i\theta} |3\rangle + e^{\frac{3}{2}i\theta} |4\rangle) \\ |4\rangle_{new} = \frac{1}{2\sqrt{2}}(e^{-\frac{3}{2}i\theta} |1\rangle - \frac{1}{\sqrt{3}}e^{-\frac{1}{2}i\theta} |2\rangle - \frac{1}{\sqrt{3}}e^{\frac{1}{2}i\theta} |3\rangle + e^{\frac{3}{2}i\theta} |4\rangle) \end{cases} \quad (2.13)$$

where  $\frac{1}{2\sqrt{2}}$  is normalization factor.

## 2.2 Selection Rules

As we want to consider transitions between energy levels through either Emission or Absorption of photons propagating from all directions and polarizations, the way is by calculating matrix elements of x,y,z components of electric dipole operator. Then we consider same transitions with an additional magnetic field.

### 2.2.1 Matrix element of electric dipole transitions

Again, a model for coupling of two level atom with electromagnetic field is what we want. Review for electric dipole approximation: when the field wavelength is much larger than the atomic size, the vector potential  $\vec{A}(\vec{r}_0 + \vec{r}, t) \simeq \vec{A}(t) \exp(ik \cdot \vec{r})$ . And the Hamiltonian that only describes interaction between atom and field can be written as:

$$H_{int} = -\frac{e}{m} \vec{p} \cdot \vec{A}(r_0, t) \quad (2.14)$$

where  $e$  and  $m$  are charge and mass of an electron. As we want to calculate electric dipole transitions between two states, final state  $|f\rangle$  and initial state  $|i\rangle$ , then it follows that

$$\langle f | H_{int} | i \rangle = -\frac{e}{m} \vec{A}(t) \langle f | \vec{p} | i \rangle \quad (2.15)$$

Also with the commutation relation  $[r, H_0] = (i\hbar\vec{p})/m$ , we can have

$$\langle f | \vec{p} | i \rangle = im\omega_{fi} \langle f | \vec{r} | i \rangle \quad (2.16)$$

where  $\vec{r} = r \sin(\theta) \cos(\phi) \vec{x} + r \sin(\theta) \sin(\phi) \vec{y} + r \cos(\theta) \vec{z}$ . Now we have two equivalent ways to calculate matrix element of the electric dipole transitions. We calculate it for quantum dot using momentum  $\vec{p}$ , but here for hydrogen atom we use the one with position  $\vec{r}$ . These matrix include the polarization information of the photon that is emitted or absorbed by an atom during the transition. This information is what we want for the selection rules.

### 2.2.2 selection rules with $\vec{B} \parallel \vec{z}$

Using states in Sec 2.1.2, and calculate  $\langle \psi_b | \vec{r} | \psi_a \rangle$ , where,  $\psi_b$  are ground states and  $\psi_a$  are first excited states (states are characterized by  $|nljm_j\rangle$ ):

$$\langle 10\frac{1}{2} \pm \frac{1}{2} | \vec{r} | 20\frac{1}{2} \pm \frac{1}{2} \rangle = 0 \quad \langle 10\frac{1}{2} \pm \frac{1}{2} | \vec{r} | 20\frac{1}{2} \mp \frac{1}{2} \rangle = 0 \quad (2.17)$$

$$\langle 10\frac{1}{2}\frac{1}{2} | \vec{r} | 21\frac{1}{2}\frac{1}{2} \rangle = -\frac{128\sqrt{6}}{729}a \begin{pmatrix} 0 \\ 0 \\ 1 \end{pmatrix} \quad \langle 10\frac{1}{2}\frac{-1}{2} | \vec{r} | 21\frac{1}{2}\frac{1}{2} \rangle = \frac{128\sqrt{6}}{729}a \begin{pmatrix} -1 \\ -i \\ 0 \end{pmatrix} \quad (2.18)$$

$$\langle 10\frac{1}{2}\frac{1}{2} | \vec{r} | 21\frac{1}{2}\frac{-1}{2} \rangle = -\frac{128\sqrt{6}}{729}a \begin{pmatrix} 1 \\ -i \\ 0 \end{pmatrix} \quad \langle 10\frac{1}{2}\frac{-1}{2} | \vec{r} | 21\frac{1}{2}\frac{-1}{2} \rangle = \frac{128\sqrt{6}}{729}a \begin{pmatrix} 0 \\ 0 \\ 1 \end{pmatrix} \quad (2.19)$$

$$\langle 10\frac{1}{2}\frac{1}{2} | \vec{r} | 21\frac{3}{2}\frac{1}{2} \rangle = \frac{256\sqrt{3}}{729}a \begin{pmatrix} 0 \\ 0 \\ 1 \end{pmatrix} \quad \langle 10\frac{1}{2}\frac{-1}{2} | \vec{r} | 21\frac{3}{2}\frac{1}{2} \rangle = \frac{128\sqrt{3}}{729}a \begin{pmatrix} -1 \\ -i \\ 0 \end{pmatrix} \quad (2.20)$$

$$\langle 10\frac{1}{2}\frac{1}{2} | \vec{r} | 21\frac{3}{2}\frac{-1}{2} \rangle = \frac{128\sqrt{3}}{729}a \begin{pmatrix} 1 \\ -i \\ 0 \end{pmatrix} \quad \langle 10\frac{1}{2}\frac{-1}{2} | \vec{r} | 21\frac{3}{2}\frac{-1}{2} \rangle = \frac{256\sqrt{3}}{729}a \begin{pmatrix} 0 \\ 0 \\ 1 \end{pmatrix} \quad (2.21)$$

$$\langle 10\frac{1}{2}\frac{1}{2} | \vec{r} | 21\frac{3}{2}\frac{3}{2} \rangle = \frac{128}{243}a \begin{pmatrix} -1 \\ -i \\ 0 \end{pmatrix} \quad \langle 10\frac{1}{2}\frac{-1}{2} | \vec{r} | 21\frac{3}{2}\frac{3}{2} \rangle = 0 \quad (2.22)$$

$$\langle 10\frac{1}{2}\frac{1}{2} | \vec{r} | 21\frac{3}{2}\frac{-3}{2} \rangle = 0 \quad \langle 10\frac{1}{2}\frac{-1}{2} | \vec{r} | 21\frac{3}{2}\frac{-3}{2} \rangle = \frac{128}{243}a \begin{pmatrix} 1 \\ -i \\ 0 \end{pmatrix} \quad (2.23)$$

where  $a$  is the Bohr radius. The vectors in above results are characterized as polarized direction of photon. It is easy to see that above transitions are satisfied with the general selection rules:

transitions are allowed when:

$$\begin{cases} \Delta l = \pm 1; \Delta m_j = 0 & \text{allowed for z- polarized light} \\ \Delta l = \pm 1; \Delta m_j = \pm 1 & \text{allowed for x- and y- polarized light} \end{cases}$$

where  $\Delta l \equiv l$  of final state  $- l$  of initial state

$\Delta m_j \equiv m_j$  of final state  $- m_j$  of initial state

and transitions are banned when:

$$\begin{cases} \Delta l = 0 & \text{or} \\ \Delta m_j = \pm 2 \end{cases}$$

### 2.2.3 selection rules with $\vec{B} \perp \vec{z}$

Using states in (2.9), (2.10), (2.11) and (2.13), and calculate matrix element of electric dipole moment: (the subscript words 'new' is omitted)

$$\langle 7|\vec{r}|1\rangle = \frac{128}{243}a \begin{pmatrix} i \sin \theta \\ -i \cos \theta \\ 1 \end{pmatrix} \quad \langle 7|\vec{r}|2\rangle = 0$$

$$\langle 7|\vec{r}|3\rangle = \frac{256}{729}\sqrt{3}a \begin{pmatrix} \cos \theta \\ \sin \theta \\ 0 \end{pmatrix} \quad \langle 7|\vec{r}|4\rangle = \frac{128}{729}\sqrt{3}a \begin{pmatrix} i \sin \theta \\ -i \cos \theta \\ -1 \end{pmatrix}$$

$$\langle 7|\vec{r}|5\rangle = \frac{256}{729}\sqrt{3}a \begin{pmatrix} -\cos \theta \\ -\sin \theta \\ 0 \end{pmatrix} \quad \langle 7|\vec{r}|6\rangle = \frac{256}{729}a \begin{pmatrix} -i \sin \theta \\ i \cos \theta \\ 1 \end{pmatrix}$$

And transitions between ground states ( $|7\rangle$ ) and states  $|9\rangle$  and  $|10\rangle$  are already banned since their  $\Delta l = 0$ .

From the result above, it can be found that polarisations are changing with  $\theta$ , where this theta coming from the external magnetic field is the rotating degree around z-axis. The selection rules are sensitive to rotation of the field this is what we expect for atom.

# Chapter 3

## Quantum Dots

In this chapter We start with a review of a simple model of a semiconductor quantum dot with zincblende structure described in book [5]. we discuss electron and hole states in a single particle model and then we calculate electric dipole transitions under an transverse magnetic field.

### 3.1 A simple model of a quantum dot

#### 3.1.1 band structure

band structure

In simplified electronic band structure of a quantum dot with zincblende structure, the energy of valence band is lower than Fermi Energy and are completely filled with electrons. And we can make a hole in v band by removing an electron. The conduction band is empty and its energy is higher than Fermi energy. Here we always consider cases at around the center of Wigner-Seitz cell(Bloch wave vector  $k = 0$ ) where energy difference of two bands are smallest. Valence band consists of light-hole (lh) band, heavy-hole (hh) band and spin-off band. Among the three sub-bands, the spin-off band has the lowest energy, and the energy gap between it and conduction band is too large for the inter-band transitions, so we exclude it from the discussion following. At  $k = 0$ , lh and hh band shared same energy and have same total angular momentum  $j = 3/2$ , but the presence of uniaxial strain gives an energy splitting between them by  $\Delta_{lh-hh}$ .

Besides, two effects contribute to band structure should be mentioned.

The energy dispersion dependent on wave vector  $k$  is contributed by effective mass of crystal electron. Holes in lh band and hh band have different effective masses, as the result, the parabolic energy dispersion of two sub-

bands have different curvature. For inter-band transitions, it should not be taken into account.

Spin-orbital interaction arises when an electron with charge moves in an external electric field, its spin couples to an experienced effective magnetic field resulting from relativistic effect. In crystal, the total angular momentum  $J$  of the electron commutes with the Hamiltonian of isotropic spin-orbital interaction, so it is good to use quantum number  $j$  to label the electron's state. Besides, in bulk crystal, small splitting contribute to spin-orbital interaction by structure inversion asymmetry in the direction perpendicular to the two-dimensional plane, and bulk inversion asymmetry of the crystal lattice, namely Rashba effect and Dresselhaus effect, are neglected in this thesis.

### 3.1.2 Carrier configuration

In this chapter we review four optically active/bright electronic states describing by carrier configurations of quantum dot in S shell. For a Qdot, when valence band is fully filled with electrons and conduction band is empty, we call it the ground state. An exciton state is formed when there are a hole in valence band and an electron in conduction band. When the electron decay to the hole, this process is the recombination of electron and hole. Recombination process only happens when spins of electron and hole are in opposite direction, otherwise the optical process is 'dark'. Positive trion is the electronic states that has two holes and one electron. Negative trion is in opposite which has two electrons but one hole. According to the pauli exclusion principle, here either electrons or holes with equal spins cannot occupy in same state, so for both two electrons in conduction band and two holes in valence band, their spin are in opposite directions. The last electronic states is called biexciton, which has two electrons and two holes. In this thesis we choose to calculate selection rules under electron-hole picture of negative trion. After the recombination process, one electron is left in the conduction band.

### 3.1.3 states of a quantum dot

In quantum dot, states of confined electrons in band  $b$  with wave vector  $k$  can be described using Bloch states  $u_k^b(r)$ , a periodic wave function in crystal potential

$$\langle r | \psi_k^b \rangle = e^{ik \cdot r} u_k^b(r) \quad (3.1)$$

Next, we only consider the case that wave vector  $k$  is almost zero, so that we can relabel the states with the total angular momentum  $j$  and its

projection  $j_z$  instead of wave vector  $k$  and band  $b$ . Then by considering orbital symmetry and spin of Bloch states, states of conduction band with orbital  $s$  symmetry can be defined as

$$|u_{+1/2}^{1/2}\rangle = |s\rangle |\uparrow\rangle \equiv |7\rangle, \quad |u_{-1/2}^{1/2}\rangle = |s\rangle |\downarrow\rangle \equiv |8\rangle \quad (3.2)$$

where spin states  $|\uparrow\rangle$  and  $|\downarrow\rangle$  is defined along axis  $z$ .

The states in valence band have orbital  $p$  symmetry. According to the Clebsch-Gordan theory, the states on heavy hole band with quantum numbers  $l = 1, s = 1/2, j = 3/2, j_z = \pm 3/2$  are defined as

$$|u_{+3/2}^{3/2}\rangle = -\frac{1}{\sqrt{2}} |x + iy\rangle |\uparrow\rangle \equiv |1\rangle \quad (3.3)$$

$$|u_{-3/2}^{3/2}\rangle = \frac{1}{\sqrt{2}} |x - iy\rangle |\downarrow\rangle \equiv |4\rangle \quad (3.4)$$

and states on light hole band with quantum numbers  $l = 1, s = 1/2, j = 3/2, j_z = \pm 1/2$  are defined as

$$|u_{+1/2}^{3/2}\rangle = -\frac{1}{\sqrt{6}} (|x + iy\rangle |\downarrow\rangle + 2|z\rangle) \equiv |2\rangle \quad (3.5)$$

$$|u_{-1/2}^{3/2}\rangle = \frac{1}{\sqrt{6}} (|x - iy\rangle |\uparrow\rangle + 2|2\rangle) \equiv |3\rangle \quad (3.6)$$

where  $|x + iy\rangle = |x\rangle \pm i|y\rangle$ , states  $|x\rangle, |y\rangle, |z\rangle$  describe orbital shape of the electron of three coordinates. Also note that states  $|1\rangle, |2\rangle, |3\rangle, |4\rangle$  are degenerate at  $k = 0$ .

### 3.1.4 bands splitting $\Delta_{lh-hh}$

Strain effect that acting on a quantum dot arises from experienced compression and extension while growing in a growth plane, for example, growing CdTe on ZnTe[7]. By considering one attribution of strain effect which splits energy degeneracy of hh and hl holes band with amount  $\Delta_{lh-hh}$  at  $k = 0$ , we obtain the Hamiltonian to be

$$H_{\Delta} = \begin{pmatrix} \Delta_{lh-hh} & 0 & 0 & 0 \\ 0 & 0 & 0 & 0 \\ 0 & 0 & 0 & 0 \\ 0 & 0 & 0 & \Delta_{lh-hh} \end{pmatrix} \quad (3.7)$$

Mathematically, treating the Hamiltonian as a perturbation, as it is diagonal, states in previous subsection can still form its eigenvectors but eigenenergies change, but we still have states degenerate on hh band and lh band.

## 3.2 Selection Rules

Consider Hamiltonian of QDt-field interaction

$$H_{int} = -\frac{q}{m_0}\vec{A}(r, t) \cdot \vec{p} - \frac{q}{m_0}\vec{S} \cdot \vec{B}(r, t) \quad (3.8)$$

The second term accounts for coupling of electron spin with magnetic part of photon and it can be neglected in dipole approximation. And in the following we use momentum  $\vec{p}$  to only calculate matrix elements of electric dipole transition between Bloch states in quantum dot as what is discussed in Sec 2.2.1.

### 3.2.1 Interband transitions

In book [5], we can obtain matrix element of electric dipole transitions by calculating  $e_{ks} \cdot \langle u_{j_z}^c | \vec{p} | u_{j_z}^v \rangle$ , where  $|u_{j_z}\rangle$  are the Bloch states in  $c$  and  $v$  band labeled by total angular momentum  $j$  and projection  $j_z$ .  $e_{ks}$  is the unit polarization vector. The semiconductor QDt with zincblende structure behold cubic symmetry, due to this property we have momentum matrix element of interband transitions between  $c$  and  $v$  bands  $\langle s | \vec{p} | \alpha \rangle$ , for  $\alpha = x, y, z$ , all equals to a constant  $p_{cv}$ , where states  $|s\rangle$  and  $|\alpha\rangle$  are orbital part of states, shown in Sec 3.1.2. With this result the matrix element of the electric dipole transition between conduction band and valence band using Eq3.2-3.6 are obtained:

$$\langle u_{+1/2}^{1/2} | \vec{p} | u_{+3/2}^{3/2} \rangle = -\frac{1}{\sqrt{2}} \begin{pmatrix} 1 \\ i \\ 0 \end{pmatrix} p_{cv} \quad \langle u_{-1/2}^{1/2} | \vec{p} | u_{-3/2}^{3/2} \rangle = \frac{1}{\sqrt{2}} \begin{pmatrix} 1 \\ -i \\ 0 \end{pmatrix} p_{cv} \quad (3.9)$$

$$\langle u_{+1/2}^{1/2} | \vec{p} | u_{-3/2}^{3/2} \rangle = \langle u_{-1/2}^{1/2} | \vec{p} | u_{+3/2}^{3/2} \rangle = 0 \quad (3.10)$$

$$\langle u_{+1/2}^{1/2} | \vec{p} | u_{-1/2}^{3/2} \rangle = \frac{1}{\sqrt{6}} \begin{pmatrix} 1 \\ -i \\ 0 \end{pmatrix} p_{cv} \quad \langle u_{-1/2}^{1/2} | \vec{p} | u_{+1/2}^{3/2} \rangle = -\frac{1}{\sqrt{6}} \begin{pmatrix} 1 \\ i \\ 0 \end{pmatrix} p_{cv} \quad (3.11)$$

$$\langle u_{+1/2}^{1/2} | \vec{p} | u_{+1/2}^{3/2} \rangle = -\frac{2}{\sqrt{6}} \begin{pmatrix} 0 \\ 0 \\ 1 \end{pmatrix} p_{cv} \quad \langle u_{-1/2}^{1/2} | \vec{p} | u_{-1/2}^{3/2} \rangle = \frac{2}{\sqrt{6}} \begin{pmatrix} 0 \\ 0 \\ 1 \end{pmatrix} p_{cv} \quad (3.12)$$

Obviously, allowed optical transitions occurs between states with same spin and same orbital symmetry. The vectors above provides information about polarization of an emitted photon. Transitions in Eq 3.9 suggest circular polarized light, but transitions in Eq 3.12 suggest only z-axis polarized

light can be detected. And the square of absolute value of these matrix element gives emission rate. Eq 3.10 are showing that transitions are blocked of all directions.

### 3.2.2 adding $\vec{B} \parallel \vec{z}$

In case placing a QDt in a magnetic field that is parallel to z-axis, Hamiltonian of the weak Zeeman effect is diagonal, so the selection rules of this situation are same as what are shown above.

### 3.2.3 adding $\vec{B} \perp \vec{z}$

In case the external magnetic field is perpendicular to z-axis, consider total perturbation Hamiltonian as:

$$H' = \mu_B B \begin{pmatrix} \tilde{\Delta}_{lh-hh} & \frac{2}{3}\sqrt{3}e^{-i\theta} & 0 & 0 \\ \frac{2}{3}\sqrt{3}e^{-i\theta} & 0 & \frac{4}{3}e^{-i\theta} & 0 \\ 0 & \frac{4}{3}e^{i\theta} & 0 & \frac{2}{3}\sqrt{3}e^{-i\theta} \\ 0 & 0 & \frac{2}{3}\sqrt{3}e^{i\theta} & \tilde{\Delta}_{lh-hh} \end{pmatrix} \quad (3.13)$$

$\tilde{\Delta}_{lh-hh} \equiv \Delta/(\mu_B B)$ . Diagonal this  $H'$ , it has eigen-energies:

$$\lambda_1 = \Delta + \frac{4(\mu_B B)^2}{3\Delta} + \frac{16(\mu_B B)^3}{9\Delta^2} \quad \lambda_2 = \frac{4}{3}\mu_B B$$

$$\lambda_3 = \Delta + \frac{4(\mu_B B)^2}{3\Delta} - \frac{16(\mu_B B)^3}{9\Delta^2} \quad \lambda_4 = \frac{4}{3}\mu_B B$$

Two eigen-energies split on high order.

In this case, transition dipole moments are:

$$\langle 7|\vec{p}|\tilde{1}\rangle = p_{cv}\alpha_1 i \begin{pmatrix} \sin\theta \\ -\cos\theta \\ 0 \end{pmatrix} \left(1 + \frac{c_1}{\sqrt{3}}\right) \quad (3.14)$$

$$\langle 7|\vec{p}|\tilde{2}\rangle = p_{cv}\alpha_2 i \begin{pmatrix} \sin\theta \\ -\cos\theta \\ 0 \end{pmatrix} \left(1 - \frac{c_2}{\sqrt{3}}\right) \quad (3.15)$$

$$\langle 7 | \vec{p} | \tilde{3} \rangle = p_{cv} \alpha_3 \begin{pmatrix} \cos \theta \\ \frac{\sin \theta}{2c_3} \\ \frac{1}{c_3 + \sqrt{3}} \end{pmatrix} \left(1 + \frac{c_3}{\sqrt{3}}\right) \quad (3.16)$$

$$\langle 7 | \vec{p} | \tilde{4} \rangle = p_{cv} \alpha_4 \begin{pmatrix} \cos \theta \\ \frac{\sin \theta}{2c_4} \\ \frac{1}{c_4 + \sqrt{3}} \end{pmatrix} \left(1 - \frac{c_4}{\sqrt{3}}\right) \quad (3.17)$$

$$\langle 8 | \vec{p} | \tilde{1} \rangle = p_{cv} \alpha_1 \begin{pmatrix} \cos \theta \\ \frac{\sin \theta}{-2c_1} \\ \frac{1}{c_1 + \sqrt{3}} \end{pmatrix} \left(1 - \frac{c_1}{\sqrt{3}}\right) \quad (3.18)$$

$$\langle 8 | \vec{p} | \tilde{2} \rangle = p_{cv} \alpha_2 \begin{pmatrix} \cos \theta \\ \frac{\sin \theta}{-2c_2} \\ \frac{1}{c_2 + \sqrt{3}} \end{pmatrix} \left(1 + \frac{c_2}{\sqrt{3}}\right) \quad (3.19)$$

$$\langle 8 | \vec{p} | \tilde{3} \rangle = p_{cv} \alpha_3 i \begin{pmatrix} \sin \theta \\ -\cos \theta \\ 0 \end{pmatrix} \left(1 - \frac{c_3}{\sqrt{3}}\right) \quad (3.20)$$

$$\langle 8 | \vec{p} | \tilde{4} \rangle = p_{cv} \alpha_4 i \begin{pmatrix} \sin \theta \\ -\cos \theta \\ 0 \end{pmatrix} \left(1 + \frac{c_4}{\sqrt{3}}\right) \quad (3.21)$$

where  $c_i$ ,  $i = 1, 2, 3, 4$  are coefficient coming from eigen-vectors:

$$c_1 = \mu_B B (4 - 3\tilde{\Delta} + \sqrt{64 - 24\tilde{\Delta} + 9\tilde{\Delta}^2}) / (4\sqrt{3})$$

$$c_2 = \mu_B B (-4 + 3\tilde{\Delta} + \sqrt{64 - 24\tilde{\Delta} + 9\tilde{\Delta}^2}) / (4\sqrt{3})$$

$$c_3 = \mu_B B (-4 - 3\tilde{\Delta} + \sqrt{64 + 24\tilde{\Delta} + 9\tilde{\Delta}^2}) / (4\sqrt{3})$$

$$c_4 = \mu_B B (4 + 3\tilde{\Delta} + \sqrt{64 + 24\tilde{\Delta} + 9\tilde{\Delta}^2}) / (4\sqrt{3})$$

and  $\alpha_i$ ,  $i = 1, 2, 3, 4$  are normalization factor defined as  $\alpha_i = \sqrt{1/(2c_i^2 + 2)}$ .

In approximation if Zeeman effect is very weak and much smaller than attribution of band splitting, mathematically by taking the limit that  $\Delta$  goes to infinite, the value of  $c_1$  and  $c_3$  are close to zero, and therefore  $\hat{z}$ -component of polarization vector of Eq3.18 and Eq3.16 will be zero.

And all of these transitions are still showing strong dependence on rotating degree of the magnetic field  $\theta$  and selection rules are very similar to the case of the hydrogen atom. For instance, Eq3.14, from  $\theta = 0$  to  $\theta = \pi/2$ , polarisation of the photon are also rotating continuously from only  $x$ - polarized light to  $y$ - polarized light.

# Chapter 4

## Regimes with $\beta$

### 4.1 Effect of Strain anistropy $\beta$

In previous chapter, we have seen that under the simple model of the quantum dot, the polarization of emitted photon caused by the atom-field interaction is highly dependent with the rotation of the field. Obviously, this result is not what we expected for, we need to consider an additional effect to fix the model of the quantum dot. As zincblende semiconductor crystal is compressed while growing in a plane[8], which gives rise to the effect of strain anistropy that acting on the valence band[7]. A simple Hamiltonian for this effect is defined as:

$$H_{str} = \beta(|p_x\rangle \langle p_x| - |p_y\rangle \langle p_y|) \quad (4.1)$$

Here  $\beta$  is a coefficient about strength of the effect. And  $|p_x\rangle$  and  $|p_y\rangle$  are orbital states along  $\hat{x}$  and  $\hat{y}$  respectively. Using the states in (Eq3.3-3.6) as basis, the matrix form of this Hamiltonian can be represented as:

$$H_{str} = \begin{pmatrix} 0 & 0 & 1 & 0 \\ 0 & 0 & 0 & 1 \\ 1 & 0 & 0 & 0 \\ 0 & 1 & 0 & 0 \end{pmatrix} \frac{-\beta}{\sqrt{3}} \quad (4.2)$$

where the Hamiltonian makes couplings between the states  $|1\rangle$  and  $|3\rangle$  and between the states  $|2\rangle$  and  $|4\rangle$ . In the following of this chapter, we do a theoretically analysis of the effect in three regimes. We use both degenerate and non-degenerate perturbation theory to obtain energy and corresponding states. Then we calculate matrix element for the electric dipole transitions. Finally we analyze how the polarization of an absorbed photon is changing in each case.

## 4.2 Regime $\Delta \gg \beta$

Now in this new model, the total strain effect include both effects of the band splitting and the strain anisotropy. In this first regime we assume that effect of the band splitting  $\Delta_{lh-hh}$  is dominant, that is to say, we treat the Hamiltonian of the band splitting  $H_\Delta$  as 'unperturbed' part and treat  $H_{str}$  as a small perturbation. Since the Hamiltonian  $H_\Delta$  is diagonal, we can use the states in Eq(3.3-3.6) as two groups of basis to get two matrix forms of the  $H_{str}$ , where the Hamiltonian makes couplings between the states  $|1\rangle$  and  $|3\rangle$  and between the states  $|2\rangle$  and  $|4\rangle$ . Therefore, we have to use the non-degenerate perturbation theory to deal with. Then we may obtain the first order perturbed states on the valence band of the following:

$$\begin{aligned} |1'\rangle &= \sqrt{1/(1+R^2/3)}(|1\rangle - (R/\sqrt{3})|3\rangle) \\ |3'\rangle &= \sqrt{1/(1+R^2/3)}(|3\rangle + (R/\sqrt{3})|1\rangle) \\ |2'\rangle &= \sqrt{1/(1+R^2/3)}(|2\rangle + (R/\sqrt{3})|4\rangle) \\ |4'\rangle &= \sqrt{1/(1+R^2/3)}(|4\rangle - (R/\sqrt{3})|2\rangle) \end{aligned}$$

where the ratio  $R \equiv \beta/\Delta$ . Not surprisingly, both states  $|1'\rangle$  and  $|4'\rangle$  also states  $|2'\rangle$  and  $|3'\rangle$  are still degenerate due to the preserved time-reversal symmetry.

By adding a magnetic field  $\vec{B} \parallel \vec{z}$ , the matrix elements for the electric dipole transitions among states on valence band and states on conduction band that are unaffected by the strain are:

$$\langle 7|\vec{p}|1'\rangle = R' \begin{pmatrix} \frac{-3-R}{3\sqrt{2}} \\ i \left( \frac{-3+R}{3\sqrt{2}} \right) \\ 0 \end{pmatrix} p_{cv} \approx R' \begin{pmatrix} 1 \\ i \\ 0 \end{pmatrix} \frac{-1}{\sqrt{2}} p_{cv} \quad (4.3)$$

$$\langle 7|\vec{p}|2'\rangle = R' \begin{pmatrix} 0 \\ 0 \\ 1 \end{pmatrix} \frac{-2}{\sqrt{6}} p_{cv} = \langle 8|\vec{p}|1'\rangle \quad (4.4)$$

$$\langle 7|\vec{p}|3'\rangle = R' \begin{pmatrix} \frac{1-R}{\sqrt{6}} \\ -i \left( \frac{1+R}{\sqrt{6}} \right) \\ 0 \end{pmatrix} p_{cv} \approx R' \begin{pmatrix} 1 \\ -i \\ 0 \end{pmatrix} \frac{1}{\sqrt{6}} p_{cv} \quad (4.5)$$

$$\langle 7|\vec{p}|4'\rangle = R' \begin{pmatrix} 0 \\ 0 \\ 1 \end{pmatrix} \frac{2}{\sqrt{6}} p_{cv} = \langle 8|\vec{p}|3'\rangle \quad (4.6)$$

$$\langle 8|\vec{p}|2'\rangle = R' \begin{pmatrix} \frac{-1+R}{\sqrt{6}} \\ -i \left( \frac{1+R}{\sqrt{6}} \right) \\ 0 \end{pmatrix} p_{cv} \approx R' \begin{pmatrix} 1 \\ i \\ 0 \end{pmatrix} \frac{-1}{\sqrt{6}} p_{cv} \quad (4.7)$$

$$\langle 8|\vec{p}|4'\rangle = R' \begin{pmatrix} \frac{3+R}{3\sqrt{2}} \\ -i \left( \frac{3-R}{3\sqrt{2}} \right) \\ 0 \end{pmatrix} p_{cv} \approx R' \begin{pmatrix} 1 \\ -i \\ 0 \end{pmatrix} \frac{1}{\sqrt{2}} p_{cv} \quad (4.8)$$

where  $R' \equiv \sqrt{1/(1+R^2/3)}$  is just a coefficient. These results are showing that when  $R$  is small, photon are circularly otherwise linearly polarized.

Now we add a magnetic field perpendicular to  $\hat{z}$  axis ( $\vec{B} \perp \vec{z}$ ), using the degenerate perturbation theory with basis  $|1'\rangle$  and  $|4'\rangle$  to obtain perturbed Hamiltonian of the Zeeman effect:

$$H_{zee} = \frac{4R}{9+3R^2} \begin{pmatrix} 0 & Re^{i\theta} - 3e^{-i\theta} \\ Re^{-i\theta} - 3e^{i\theta} & 0 \end{pmatrix} \quad (4.9)$$

The eigenvalues of the above Hamiltonian are:

$$\begin{aligned} \mp (4/\sqrt{3})Re^{-i\theta} \sqrt{-R + 3e^{2i\theta} + R^2e^{2i\theta}/3 - Re^{4i\theta}} \mu_B B / (3 + R^2) \\ = (4R[(-2R \cos 2\theta)/3 + 1 + R^2/9]^{1/2}) \mu_B B / (3 + R^2) \end{aligned}$$

Now we redo the same step with basis  $|2'\rangle$  and  $|3'\rangle$ , we obtain:

$$H_{zee} = \frac{4}{3+R^2} \begin{pmatrix} 0 & e^{-i\theta} + Re^{i\theta} \\ e^{i\theta} + Re^{-i\theta} & 0 \end{pmatrix} \quad (4.10)$$

And its eigenvalues are:

$$\begin{aligned} \mp 4e^{-i\theta} \sqrt{R + e^{2i\theta} + R^2e^{2i\theta} + Re^{4i\theta}} \mu_B B / (3 + R^2) \\ = 4[2R \cos 2\theta + 1 + R^2]^{1/2} \mu_B B / (3 + R^2) \end{aligned}$$

The plot of the g-factor, the eigenvalues above divided by  $\mu_B B$ , are shown in Fig4.1.

By diagonalizing Hamiltonian in Eq4.9 and Eq4.10, we also obtain their eigenstates, that is, the wave function of electrons on valence band.

$$\begin{cases} |1'_{zee}\rangle = \sqrt{1/(|L_1(\theta)|^2 + 1)}(L_1(\theta) |1'\rangle + |4'\rangle) \\ |2'_{zee}\rangle = \sqrt{1/(|L_1(\theta)|^2 + 1)}(-L_1(\theta) |1'\rangle + |4'\rangle) \\ |3'_{zee}\rangle = \sqrt{1/(|L_2(\theta)|^2 + 1)}(L_2(\theta) |2'\rangle + |3'\rangle) \\ |4'_{zee}\rangle = \sqrt{1/(|L_2(\theta)|^2 + 1)}(-L_2(\theta) |2'\rangle + |3'\rangle) \end{cases}$$

where  $L_1(\theta) = \sqrt{-R + (3 + R^2/3)e^{2i\theta} - Re^{4i\theta}}/(-R/\sqrt{3} + \sqrt{3}e^{2i\theta})$  and  $L_2(\theta) = -\sqrt{R + (1 + R^2)e^{2i\theta} + Re^{4i\theta}}/(R + e^{2i\theta})$

And states on conduction band are:

$$|7_{zee}\rangle = (e^{i\theta/2} |7\rangle + e^{-i\theta/2} |8\rangle)/\sqrt{2} \quad |8_{zee}\rangle = (-e^{i\theta/2} |7\rangle + e^{-i\theta/2} |8\rangle)/\sqrt{2}$$

Again, we calculate the matrix elements for the electric dipole transitions:

$$\langle 7_{zee} | \vec{p} | 1'_{zee} \rangle = \frac{p_{cv}}{\sqrt{2}} R' \sqrt{\frac{1}{|L_1(\theta)|^2 + 1}} \begin{pmatrix} \frac{3+R}{3\sqrt{2}} ([-L_1(\theta) e^{i\theta/2} + e^{-i\theta/2}]) \\ i \left( \frac{-3+R}{3\sqrt{2}} \right) [L_1(\theta) e^{i\theta/2} + e^{-i\theta/2}] \\ (e^{i\theta/2} - L_1(\theta) e^{-i\theta/2}) \frac{2}{3\sqrt{2}} R \end{pmatrix}$$

$$\langle 7_{zee} | \vec{p} | 2'_{zee} \rangle = \frac{p_{cv}}{\sqrt{2}} R' \sqrt{\frac{1}{|L_1(\theta)|^2 + 1}} \begin{pmatrix} \frac{3+R}{3\sqrt{2}} ([L_1(\theta) e^{i\theta/2} + e^{-i\theta/2}]) \\ i \left( \frac{-3+R}{3\sqrt{2}} \right) [-L_1(\theta) e^{i\theta/2} + e^{-i\theta/2}] \\ (e^{i\theta/2} + L_1(\theta) e^{-i\theta/2}) \frac{2}{3\sqrt{2}} R \end{pmatrix}$$

$$\langle 7_{zee} | \vec{p} | 3'_{zee} \rangle = \frac{p_{cv}}{\sqrt{2}} R' \sqrt{\frac{1}{|L_2(\theta)|^2 + 1}} \begin{pmatrix} \frac{1-R}{\sqrt{6}} ([-L_2(\theta) e^{-i\theta/2} + e^{i\theta/2}]) \\ -i \left( \frac{1+R}{\sqrt{6}} \right) [L_2(\theta) e^{-i\theta/2} + e^{i\theta/2}] \\ (e^{-i\theta/2} - L_2(\theta) e^{i\theta/2}) \frac{2}{\sqrt{6}} \end{pmatrix}$$

$$\langle 7_{zee} | \vec{p} | 4'_{zee} \rangle = \frac{p_{cv}}{\sqrt{2}} R' \sqrt{\frac{1}{|L_2(\theta)|^2 + 1}} \begin{pmatrix} \frac{1-R}{\sqrt{6}} ([L_2(\theta) e^{-i\theta/2} + e^{i\theta/2}]) \\ -i \left( \frac{1+R}{\sqrt{6}} \right) [-L_2(\theta) e^{-i\theta/2} + e^{i\theta/2}] \\ (e^{-i\theta/2} + L_2(\theta) e^{i\theta/2}) \frac{2}{\sqrt{6}} \end{pmatrix}$$

$$\begin{aligned}
\langle 8_{zee} | \vec{p} | 1'_{zee} \rangle &= \frac{p_{cv}}{\sqrt{2}} R' \sqrt{\frac{1}{|L_1(\theta)|^2 + 1}} \left( \begin{array}{c} \frac{3+R}{3\sqrt{2}} ([L_1(\theta) e^{i\theta/2} + e^{-i\theta/2}]) \\ i \left( \frac{-3+R}{3\sqrt{2}} \right) [-L_1(\theta) e^{i\theta/2} + e^{-i\theta/2}] \\ - (e^{i\theta/2} + L_1(\theta) e^{-i\theta/2}) \frac{2}{3\sqrt{2}} R \end{array} \right) \\
\langle 8_{zee} | \vec{p} | 2'_{zee} \rangle &= \frac{p_{cv}}{\sqrt{2}} R' \sqrt{\frac{1}{|L_1(\theta)|^2 + 1}} \left( \begin{array}{c} \frac{3+R}{3\sqrt{2}} ([-L_1(\theta) e^{i\theta/2} + e^{-i\theta/2}]) \\ i \left( \frac{-3+R}{3\sqrt{2}} \right) [L_1(\theta) e^{i\theta/2} + e^{-i\theta/2}] \\ - (e^{i\theta/2} - L_1(\theta) e^{-i\theta/2}) \frac{2}{3\sqrt{2}} R \end{array} \right) \\
\langle 8_{zee} | \vec{p} | 3'_{zee} \rangle &= \frac{p_{cv}}{\sqrt{2}} R' \sqrt{\frac{1}{|L_2(\theta)|^2 + 1}} \left( \begin{array}{c} \frac{1-R}{\sqrt{6}} ([-L_2(\theta) e^{-i\theta/2} - e^{i\theta/2}]) \\ -i \left( \frac{1+R}{\sqrt{6}} \right) [L_2(\theta) e^{-i\theta/2} - e^{i\theta/2}] \\ (e^{-i\theta/2} + L_2(\theta) e^{i\theta/2}) \frac{2}{\sqrt{6}} \end{array} \right) \\
\langle 8_{zee} | \vec{p} | 4'_{zee} \rangle &= \frac{p_{cv}}{\sqrt{2}} R' \sqrt{\frac{1}{|L_2(\theta)|^2 + 1}} \left( \begin{array}{c} \frac{1-R}{\sqrt{6}} ([L_2(\theta) e^{-i\theta/2} - e^{i\theta/2}]) \\ -i \left( \frac{1+R}{\sqrt{6}} \right) [-L_2(\theta) e^{-i\theta/2} - e^{i\theta/2}] \\ (e^{-i\theta/2} - L_2(\theta) e^{i\theta/2}) \frac{2}{\sqrt{6}} \end{array} \right)
\end{aligned}$$

Now, for the sake of convenience, we define a function  $\Gamma$ .

$$\Gamma = |\langle f | \vec{p} | i \rangle \hat{x}|^2 \quad (4.11)$$

and

$$\Gamma_{xy} = (1/2) |\langle f | \vec{p} | i \rangle (\hat{x} + \hat{y})|^2 \quad (4.12)$$

where  $|f\rangle$  and  $|i\rangle$  are states on conduction band, and on valence band respectively. Clearly, function  $\Gamma$  describes the rate of photon absorption with polarization along  $\hat{x}$  axis. Also in order to simulate a 45 degree waveguide on  $\hat{x}\hat{y}$  plane, we defined  $\Gamma_{xy}$ . The plots of functions  $\Gamma$  and  $\Gamma_{xy}$  (fig.4.2), are showing variation of the polarization against rotation degree of the field. Lines in graphs (a) and (b) are almost straight, which denotes very weak dependence on rotation of the magnetic field. And  $\hat{x}$ -polarized light for transitions in (a) are blocked, but  $\hat{y}$ -polarized light are allowed. And in (b), the situation is opposite, But for figure (c) and (d), we see that polarization

are changing sinusoidally, compared to (a) and (b), these variations are much more intensive. And we do not plot transitions with state  $|8\rangle$ , as we will see the same plots due to the time reversal symmetry.

### 4.3 limit $\beta \gg \Delta$

Again, in this subsection we redo similar steps as before for the case effect of strain anisotropy is dominant, that is, the  $R$  is large. We start with states of Eq(3.3-3.6) as two groups of coupled basis, and apply the degenerate perturbation theory twice. We first treat  $H_{str}$  as a small perturbation acting on the states, then following by another small perturbation due to  $H_{\Delta}$ . In the end, we may obtain the perturbed states of the following:

$$|1''\rangle = (|2\rangle + |4\rangle)/\sqrt{2} \quad |2''\rangle = (|1\rangle + |3\rangle)/\sqrt{2} \quad (4.13)$$

$$|3''\rangle = (-|2\rangle + |4\rangle)/\sqrt{2} \quad |4''\rangle = (-|1\rangle + |3\rangle)/\sqrt{2} \quad (4.14)$$

Unlike the case in previous regime, these states are independent of  $R$ . States  $|1''\rangle$  and  $|2''\rangle$  are degenerate with corresponding energy equals to  $(1/2)\Delta - \beta/\sqrt{3}$ . Also states  $|3''\rangle$  and  $|4''\rangle$  are degenerate with corresponding energy equals to  $(1/2)\Delta + \beta/\sqrt{3}$ .

Then matrix element of electric dipole transitions with magnetic field parallel to z-axis can be reached.

$$\langle 7|\vec{p}|1''\rangle = \frac{-1}{\sqrt{3}} \begin{pmatrix} 0 \\ 0 \\ 1 \end{pmatrix} p_{cv} \quad \langle 8|\vec{p}|1''\rangle = \frac{\sqrt{3}}{6} \begin{pmatrix} \sqrt{3}-1 \\ -i(\sqrt{3}+1) \\ 0 \end{pmatrix} p_{cv}$$

$$\langle 7|\vec{p}|2''\rangle = \frac{\sqrt{3}}{6} \begin{pmatrix} -\sqrt{3}+1 \\ -i(\sqrt{3}+1) \\ 0 \end{pmatrix} p_{cv} \quad \langle 8|\vec{p}|2''\rangle = \frac{1}{\sqrt{3}} \begin{pmatrix} 0 \\ 0 \\ 1 \end{pmatrix} p_{cv}$$

$$\langle 7|\vec{p}|3''\rangle = \frac{1}{\sqrt{3}} \begin{pmatrix} 0 \\ 0 \\ 1 \end{pmatrix} p_{cv} \quad \langle 8|\vec{p}|3''\rangle = \frac{\sqrt{3}}{6} \begin{pmatrix} \sqrt{3}+1 \\ i(-\sqrt{3}+1) \\ 0 \end{pmatrix} p_{cv}$$

$$\langle 7|\vec{p}|4''\rangle = \frac{\sqrt{3}}{6} \begin{pmatrix} \sqrt{3}+1 \\ i(\sqrt{3}-1) \\ 0 \end{pmatrix} p_{cv} \quad \langle 8|\vec{p}|4''\rangle = \frac{1}{\sqrt{3}} \begin{pmatrix} 0 \\ 0 \\ 1 \end{pmatrix} p_{cv}$$

The results above are noting fresh. Now we reconsider to add the magnetic field perpendicular to z-axis. consider coupling between states  $|1''\rangle$  and

$|2''\rangle$  are connected by the field.

$$H_{zee} = \begin{pmatrix} 0 & \frac{2}{3}\sqrt{3}e^{i\theta} + \frac{2}{3}e^{-i\theta} \\ \frac{2}{3}\sqrt{3}e^{-i\theta} + \frac{2}{3}e^{i\theta} & 0 \end{pmatrix} \mu_B B \quad (4.15)$$

its eigenvalues are

$$\mp \frac{2}{3}e^{-i\theta} \sqrt{4e^{2i\theta} + \sqrt{3}e^{4i\theta} + \sqrt{3}\mu_B B}$$

And for the coupling between states  $|3''\rangle$  and  $|4''\rangle$

$$H_{zee} = \begin{pmatrix} 0 & \frac{2}{3}\sqrt{3}e^{i\theta} - \frac{2}{3}e^{-i\theta} \\ \frac{2}{3}\sqrt{3}e^{-i\theta} - \frac{2}{3}e^{i\theta} & 0 \end{pmatrix} \mu_B B \quad (4.16)$$

the eigenvalues are

$$\mp \frac{2}{3}e^{-i\theta} \sqrt{4e^{2i\theta} - \sqrt{3}e^{4i\theta} - \sqrt{3}\mu_B B}$$

Now we can make a plot of g factor, namely, eigenvectors divided by  $\mu_B B$ . Fig(4.3) are showing that g factor is changing periodically against  $\theta$ , which behaving like a spin 1/2 particle.

The corresponding eigenstates are

$$\begin{cases} |1''_{zee}\rangle = (f_1(\theta) |1''\rangle + |2''\rangle) / \sqrt{|f_1(\theta)|^2 + 1} \\ |2''_{zee}\rangle = (f_2(\theta) |1''\rangle + |2''\rangle) / \sqrt{|f_2(\theta)|^2 + 1} \\ |3''_{zee}\rangle = (f_3(\theta) |3''\rangle + |4''\rangle) / \sqrt{|f_3(\theta)|^2 + 1} \\ |4''_{zee}\rangle = (f_4(\theta) |3''\rangle + |4''\rangle) / \sqrt{|f_4(\theta)|^2 + 1} \end{cases}$$

where  $f_1 = -f_2 = -\sqrt{4e^{2i\theta} + \sqrt{3}e^{4i\theta} + \sqrt{3}} / (\sqrt{3} + e^{2i\theta})$

$f_3 = -f_4 = -\sqrt{4e^{2i\theta} - \sqrt{3}e^{4i\theta} - \sqrt{3}} / (\sqrt{3} - e^{2i\theta})$

Then again we calculate matrix element of dipole transitions

$$\langle 7_{zee} | \vec{p} | 1''_{zee} \rangle = \frac{p_{cv}}{\sqrt{6}} \frac{1}{\sqrt{|f_1(\theta)|^2 + 1}} \begin{pmatrix} (-\sqrt{3} + 1)(e^{i\theta/2} - e^{-i\theta/2} f_1)/2 \\ i((-\sqrt{3} - 1)(e^{i\theta/2} + e^{-i\theta/2} f_1)/2) \\ e^{-i\theta/2} - e^{i\theta/2} f_1 \end{pmatrix}$$

$$\langle 7_{zee} | \vec{p} | 2''_{zee} \rangle = \frac{p_{cv}}{\sqrt{6}} \frac{1}{\sqrt{|f_2(\theta)|^2 + 1}} \begin{pmatrix} (-\sqrt{3} + 1)(e^{i\theta/2} - e^{-i\theta/2} f_2)/2 \\ i((-\sqrt{3} - 1)(e^{i\theta/2} + e^{-i\theta/2} f_2)/2) \\ e^{-i\theta/2} - e^{i\theta/2} f_2 \end{pmatrix}$$

$$\begin{aligned}
\langle 7_{zee} | \vec{p} | 3''_{zee} \rangle &= \frac{p_{cv}}{\sqrt{6}} \frac{1}{\sqrt{|f_3(\theta)^2| + 1}} \begin{pmatrix} (\sqrt{3} + 1)(e^{i\theta/2} + e^{-i\theta/2} f_3)/2 \\ i((\sqrt{3} - 1)(e^{i\theta/2} - e^{-i\theta/2} f_3)/2) \\ e^{-i\theta/2} + e^{i\theta/2} f_3 \end{pmatrix} \\
\langle 7_{zee} | \vec{p} | 4''_{zee} \rangle &= \frac{p_{cv}}{\sqrt{6}} \frac{1}{\sqrt{|f_4(\theta)^2| + 1}} \begin{pmatrix} (\sqrt{3} + 1)(e^{i\theta/2} + e^{-i\theta/2} f_4)/2 \\ i((\sqrt{3} - 1)(e^{i\theta/2} - e^{-i\theta/2} f_4)/2) \\ e^{-i\theta/2} + e^{i\theta/2} f_4 \end{pmatrix} \\
\langle 8_{zee} | \vec{p} | 1''_{zee} \rangle &= \frac{p_{cv}}{\sqrt{6}} \frac{1}{\sqrt{|f_1(\theta)^2| + 1}} \begin{pmatrix} (\sqrt{3} - 1)(e^{i\theta/2} + e^{-i\theta/2} f_1)/2 \\ i((-\sqrt{3} - 1)(-e^{i\theta/2} + e^{-i\theta/2} f_1)/2) \\ e^{-i\theta/2} + e^{i\theta/2} f_1 \end{pmatrix} \\
\langle 8_{zee} | \vec{p} | 2''_{zee} \rangle &= \frac{p_{cv}}{\sqrt{6}} \frac{1}{\sqrt{|f_2(\theta)^2| + 1}} \begin{pmatrix} (\sqrt{3} - 1)(e^{i\theta/2} + e^{-i\theta/2} f_2)/2 \\ i((-\sqrt{3} - 1)(-e^{i\theta/2} + e^{-i\theta/2} f_2)/2) \\ e^{-i\theta/2} + e^{i\theta/2} f_2 \end{pmatrix} \\
\langle 8_{zee} | \vec{p} | 3''_{zee} \rangle &= \frac{p_{cv}}{\sqrt{6}} \frac{1}{\sqrt{|f_3(\theta)^2| + 1}} \begin{pmatrix} (\sqrt{3} + 1)(-e^{i\theta/2} + e^{-i\theta/2} f_3)/2 \\ i((1 - \sqrt{3})(e^{i\theta/2} + e^{-i\theta/2} f_3)/2) \\ e^{-i\theta/2} - e^{i\theta/2} f_3 \end{pmatrix} \\
\langle 8_{zee} | \vec{p} | 4''_{zee} \rangle &= \frac{p_{cv}}{\sqrt{6}} \frac{1}{\sqrt{|f_4(\theta)^2| + 1}} \begin{pmatrix} (\sqrt{3} + 1)(-e^{i\theta/2} + e^{-i\theta/2} f_4)/2 \\ i((1 - \sqrt{3})(e^{i\theta/2} + e^{-i\theta/2} f_4)/2) \\ e^{-i\theta/2} - e^{i\theta/2} f_4 \end{pmatrix}
\end{aligned}$$

The gamma functions are plotted in Fig4.4. In this regime, the variation of polarization of the photon is very irregular compared to the regime of small R. In the figure (a),  $x$ - polarized light is allowed but insensitive to the rotation of the magnetic field, and polarization of  $y$ - direction is changing much larger. There is one wired thing by looking at  $\Gamma_{xy}$ , from  $\theta = 0.2\pi$  to  $\theta = 0.4\pi$ , it seems that polarization of  $x$ - and  $y$ - direction cancel each other. Similar thing also happens in same region of  $\theta$  of the figure (c). In (b) and (d), we also observe irregular variation of  $\Gamma_{xy}$ . These phenomenon are probably the result of dominant effect of strain anisotropy. Besides, it is easy to observe that  $x$ - polarized light is almost banned in transition (b), and  $y$ - polarized light is almost banned in the transition (d).

## 4.4 overall regime

In this section we do approximation in overall regime that include both small R and big R. We start by consider Hamiltonian

$$H = \begin{pmatrix} \Delta & -\beta/3 \\ -\beta/3 & 0 \end{pmatrix} \quad (4.17)$$

acting on the states  $|1\rangle, |3\rangle$

and

$$H = \begin{pmatrix} 0 & -\beta/3 \\ -\beta/3 & \Delta \end{pmatrix} \quad (4.18)$$

acting on the states  $|2\rangle, |4\rangle$

To diagonalize them we get eigenvalues  $(3\Delta \pm \sqrt{3}\sqrt{3\Delta^2 + 4\beta^2})/6$  and new states

$$\begin{cases} |1^*\rangle = (q_1 |1\rangle + |3\rangle) \sqrt{1/(q_1^2 + 1)} \\ |2^*\rangle = (q_2 |1\rangle + |3\rangle) \sqrt{1/(q_2^2 + 1)} \\ |3^*\rangle = (q_3 |2\rangle + |4\rangle) \sqrt{1/(q_3^2 + 1)} \\ |4^*\rangle = (q_4 |2\rangle + |4\rangle) \sqrt{1/(q_4^2 + 1)} \end{cases}$$

where

$$q_1 = (-\sqrt{3}\Delta + \sqrt{3\Delta^2 + 4\beta^2})/(2\beta) = (-\sqrt{3} + \sqrt{3 + 4R^2})/(2R)$$

$$q_2 = (-\sqrt{3}\Delta - \sqrt{3\Delta^2 + 4\beta^2})/(2\beta) = (-\sqrt{3} - \sqrt{3 + 4R^2})/(2R)$$

$$q_3 = (\sqrt{3}\Delta + \sqrt{3\Delta^2 + 4\beta^2})/(2\beta) = (\sqrt{3} + \sqrt{3 + 4R^2})/(2R)$$

$$q_4 = (\sqrt{3}\Delta - \sqrt{3\Delta^2 + 4\beta^2})/(2\beta) = (\sqrt{3} - \sqrt{3 + 4R^2})/(2R)$$

are elements of the eigenvectors.

Still we have states  $|1\rangle$  and  $|3\rangle$  degenerate, also states  $|2\rangle$  and  $|4\rangle$  are degenerate. By adding the magnetic field perpendicular to z-axis and using the degenerate perturbation theory. we derive the states for the perturbed system:

for the Hamiltonian of the Zeeman effect using  $|1\rangle$  and  $|3\rangle$  as basis, eigenvalues are approximately: (only for  $\theta$  from  $-0.5\pi$  to  $0.5\pi$ )

$$\mp (1/(9R^4)) \sqrt{R^4/(48R^2 + 64R^4)} \times [(4608R^5 + 1536\sqrt{9 + 12R^2}R^5 + 6144R^7 + 2048\sqrt{9 + 12R^2}R^7) \times (2 \cos(2\theta) + 1/R) + 12288R^6 + 16384R^8]^{1/2} \times \mu_B B / (48R^2 + 64R^4)$$

and the corresponded eigenstates are:

$$\begin{cases} |1_{zee}^*\rangle = \sqrt{1/(|k_1|^2 + 1)}(k_1 |1^*\rangle + |3^*\rangle) \\ |2_{zee}^*\rangle = \sqrt{1/(|k_2|^2 + 1)}(k_2 |1^*\rangle + |3^*\rangle) \end{cases}$$

where

$$k_1 = -k_2 = -[2R^2(3R + \sqrt{9 + 12R^2}R + (3 + 8R^2 + \sqrt{9 + 12R^2})e^{2i\theta} + (3R + \sqrt{9 + 12R^2})e^{4i\theta})]^{1/2} / [R(\sqrt{3} + \sqrt{3 + 4R^2} + 2\sqrt{3}Re^{2i\theta})]$$

for the Hamiltonian of the Zeeman effect using  $|2\rangle$  and  $|4\rangle$  as basis, eigenvalues are approximately: (only for  $\theta$  from  $-0.5\pi$  to  $0.5\pi$ )

$$\mp (1/(9R^4))\sqrt{R^4/(48R^2 + 64R^4)} \times [(4608R^5 - 1536\sqrt{9 + 12R^2}R^5 + 6144R^7 - 2048\sqrt{9 + 12R^2}R^7) \times (2 \cos(2\theta) + 1/R) + 12288R^6 + 16384R^8]^{1/2} \times \mu_B B / (48R^2 + 64R^4)$$

and the corresponded states are:

$$\begin{cases} |3_{zee}^*\rangle = \sqrt{1/(|k_3|^2 + 1)}(k_3 |2^*\rangle + |4^*\rangle) \\ |4_{zee}^*\rangle = \sqrt{1/(|k_4|^2 + 1)}(k_4 |2^*\rangle + |4^*\rangle) \end{cases}$$

where

$$k_3 = -k_4 = -[-2R^2(-3R + \sqrt{9 + 12R^2}R + (-3 - 8R^2 + \sqrt{q + 12R^2})e^{2i\theta} + (-3R + \sqrt{9 + 12R^2})e^{4i\theta})]^{1/2} / [R(\sqrt{3} - \sqrt{3 + 4R^2} + 2\sqrt{3}Re^{2i\theta})]$$

And the matrix element of the dipole transition in this overall regime are

$$\langle 7_{zee} | \vec{p} | X_{zee}^* \rangle = p_{cv} \sqrt{1/(2|k_X|^2 + 2)} \times \begin{pmatrix} k_X \sqrt{1/(|q_Y|^2 + 1)} e^{i\theta/2} (1/\sqrt{3} - q_Y) + \sqrt{1/(|q_Z|^2 + 1)} e^{-i\theta/2} (1 - q_Z/\sqrt{3}) \\ i[k_X \sqrt{1/(|q_Y|^2 + 1)} e^{i\theta/2} (-1/\sqrt{3} - q_Y) + \sqrt{1/(|q_Z|^2 + 1)} e^{-i\theta/2} (-1 - q_Z/\sqrt{3})] \\ 2[\sqrt{1/(|q_Z|^2 + 1)} e^{i\theta/2} (-q_Z) + k_X \sqrt{1/(|q_Y|^2 + 1)} e^{-i\theta/2}] / \sqrt{3} \end{pmatrix}$$

$$\langle 8_{zee} | \vec{p} | X_{zee}^* \rangle = p_{cv} \sqrt{1/(2|k_X|^2 + 2)} \times \begin{pmatrix} k_X \sqrt{1/(|q_Y|^2 + 1)} e^{i\theta/2} (q_Y - 1/\sqrt{3}) + \sqrt{1/(|q_Z|^2 + 1)} e^{-i\theta/2} (1 - q_Z/\sqrt{3}) \\ i[k_X \sqrt{1/(|q_Y|^2 + 1)} e^{i\theta/2} (1/\sqrt{3} + q_Y) + \sqrt{1/(|q_Z|^2 + 1)} e^{-i\theta/2} (-1 - q_Z/\sqrt{3})] \\ 2[\sqrt{1/(|q_Z|^2 + 1)} e^{i\theta/2} (q_Z) + k_X \sqrt{1/(|q_Y|^2 + 1)} e^{-i\theta/2}] / \sqrt{3} \end{pmatrix}$$

where  $|X_{zee}^*\rangle$  are states on valence band. Specifically, we compressed the total eight transitions into above form.

$$\begin{cases} X = 1; Y = 1, Z = 3 \\ X = 2; Y = 1, Z = 3 \\ X = 3; Y = 2, Z = 4 \\ X = 4; Y = 2, Z = 4 \end{cases}$$

And the total eight transitions can be reverted by replace X,Y,Z into numbers as the cases above. And the plot of the gamma function are shown in Fig4.6,4.7,4.8,4.9. Also the plot of the g-factor in this overall regime are shown in Fig4.5. Generally, the  $\Gamma$  functions and g-factors in previous two regime are in accordance with the result in this overall regime.

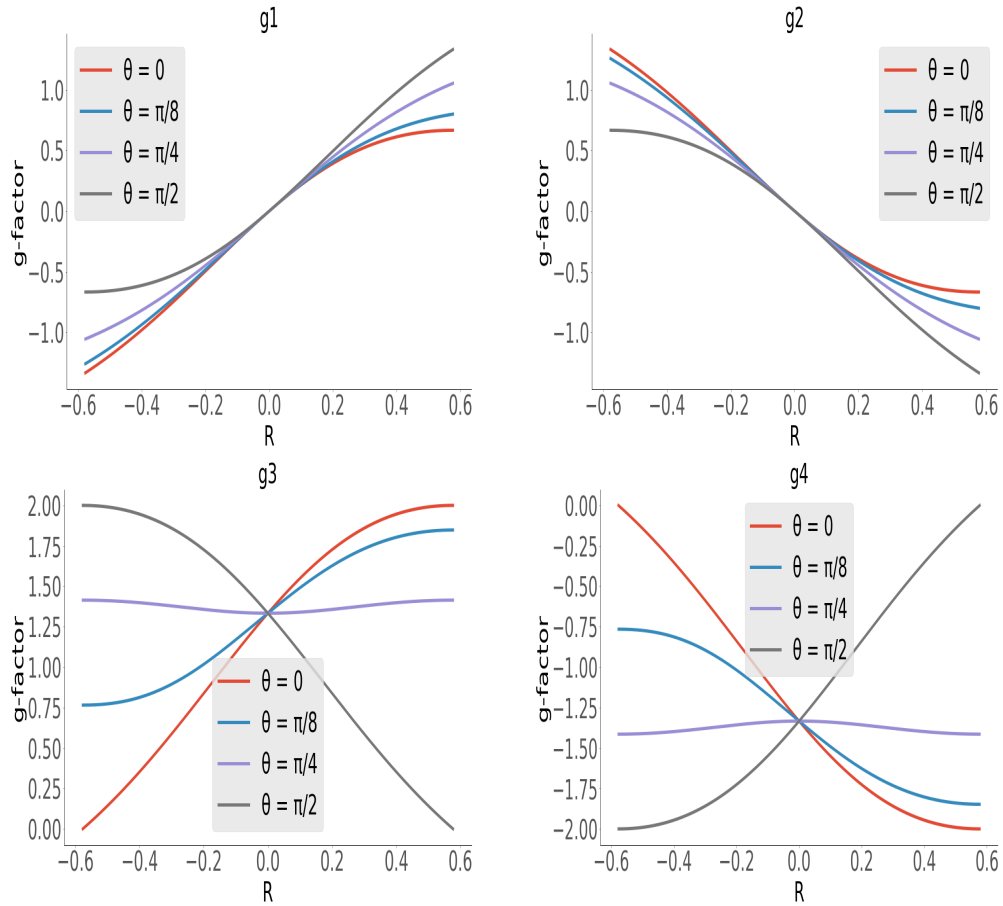


Figure 4.1: plot g1 and g2 are plot of eigenvalues of Eq4.9 divided by  $\mu_B B$ , namely, the so called g factor. And g3 and g4 are g factor of Eq4.10. An important fact is shown that when R is close to zero, g1, g2 are weakly dependent on rotation of external magnetic field, which is unlike the case we see for Hydrogen. But for g3 and g4, their dependence on  $\theta$  are changing more obviously sensitive to the variation of value of R.

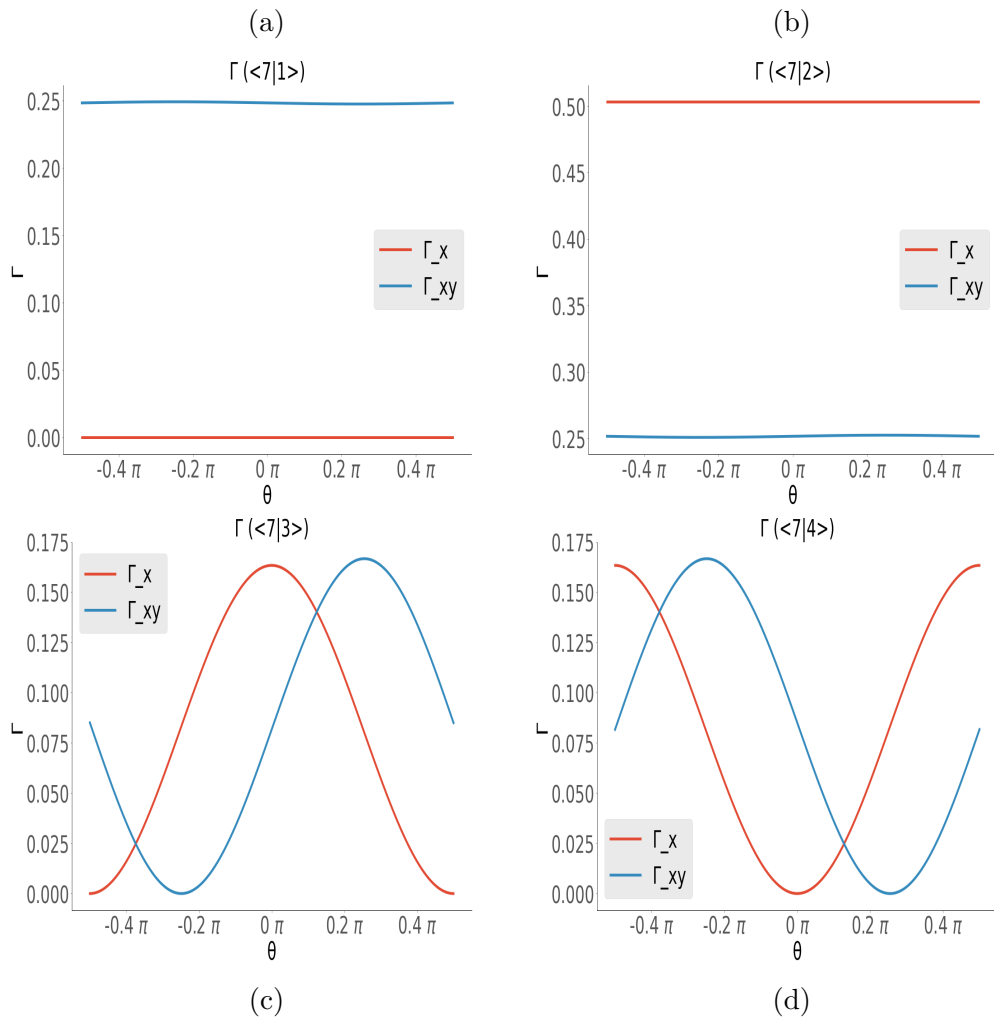


Figure 4.2: Plot of function  $\Gamma$  in regime of small  $R$ .

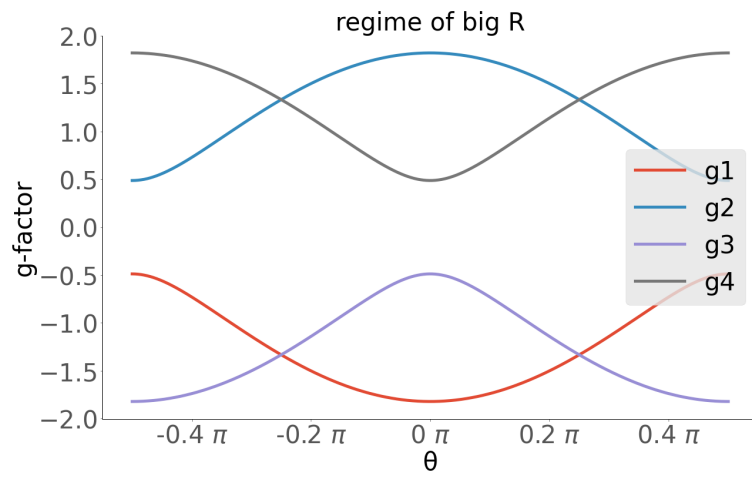


Figure 4.3: g-factor in the regime of big R. g1 and g2 are eigenvalues of Eq4.15 divided by  $\mu_B B$ , g3 and g4 are that of Eq4.16

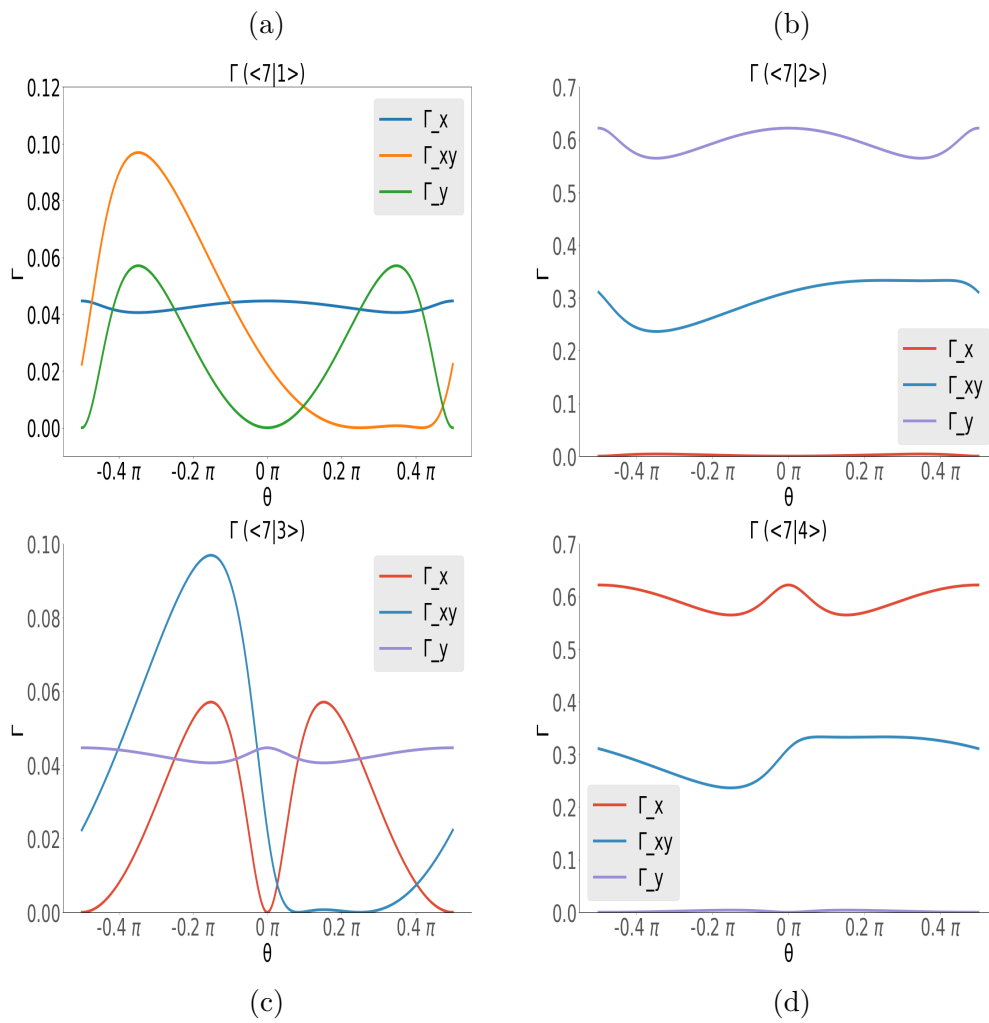


Figure 4.4: Plot of the gamma function in the regime of big R

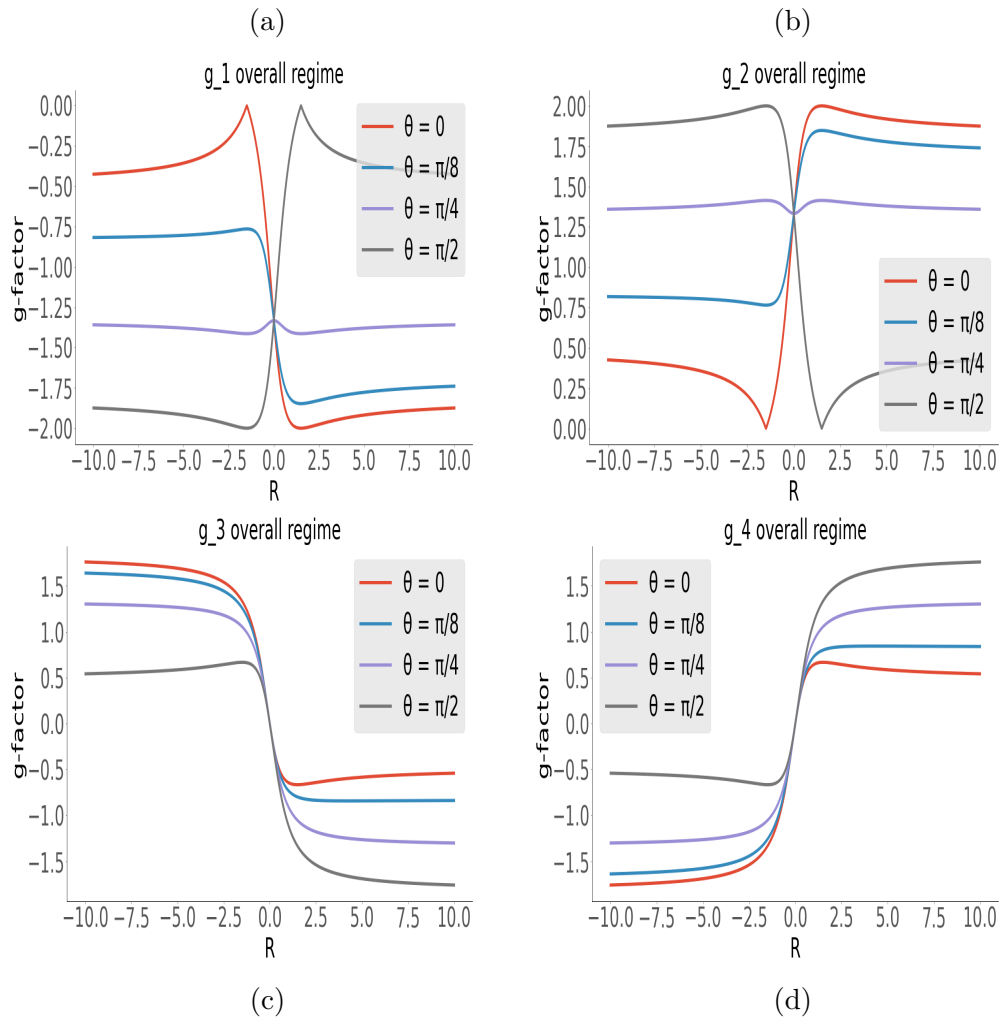


Figure 4.5: Plot of g-factor in overall regime. (a) corresponds to Fig4.1 g4 and Fig4.3 g1; (b) corresponds to Fig4.1 g3 and Fig4.3 g2; (c) corresponds to Fig4.1 g2 and Fig4.3 g3; (d) corresponds to Fig4.1 g1 and Fig4.3 g4

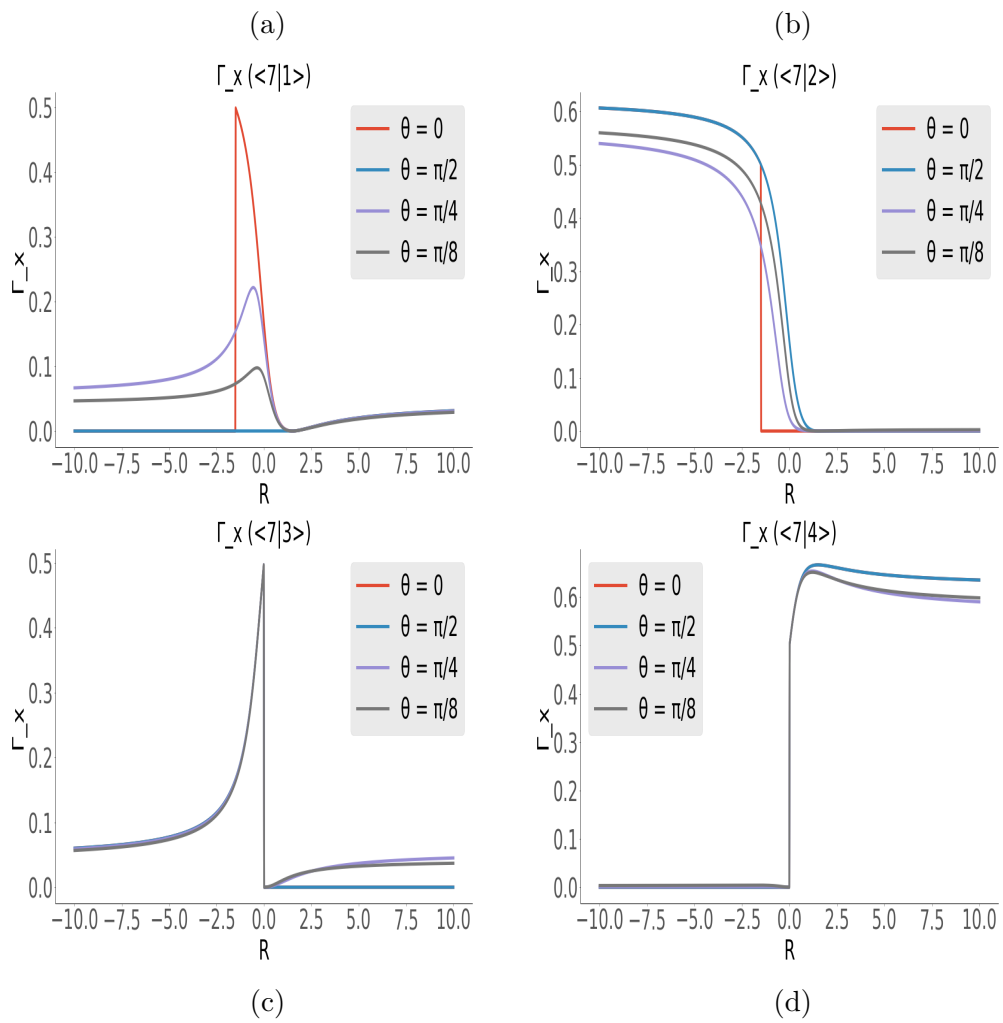


Figure 4.6: Plot of function  $\Gamma_x$  vs  $R$  in the overall regime.

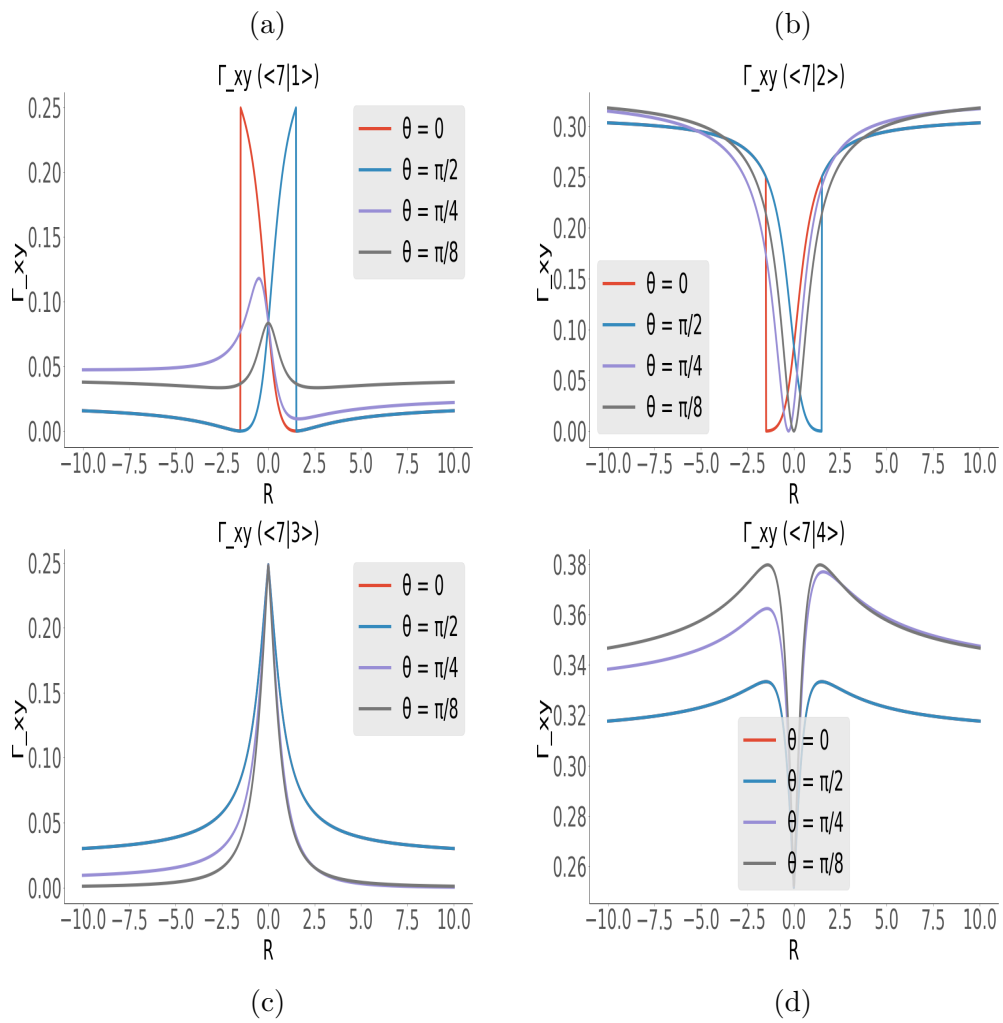


Figure 4.7: Plot of function  $\Gamma_{xy}$  vs R in the overall regime

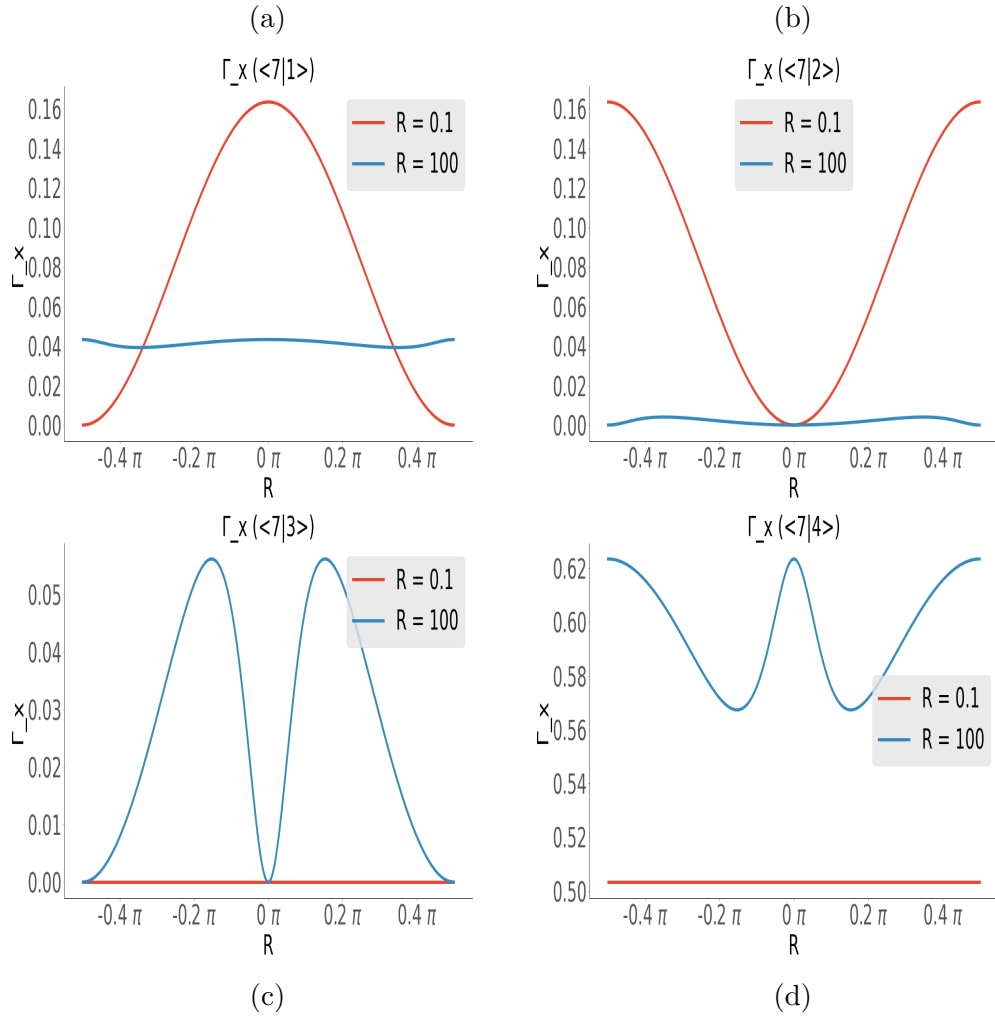


Figure 4.8: Plot of function  $\Gamma_x$  vs theta in the overall regime. (a) corresponds to Fig4.2 (c) and Fig4.4 (a); (b) corresponds to Fig4.2 (d) and Fig4.4 (b); (c) corresponds to Fig4.2 (a) and Fig4.4 (c); (d) corresponds to Fig4.2 (b) and Fig4.4 (d)

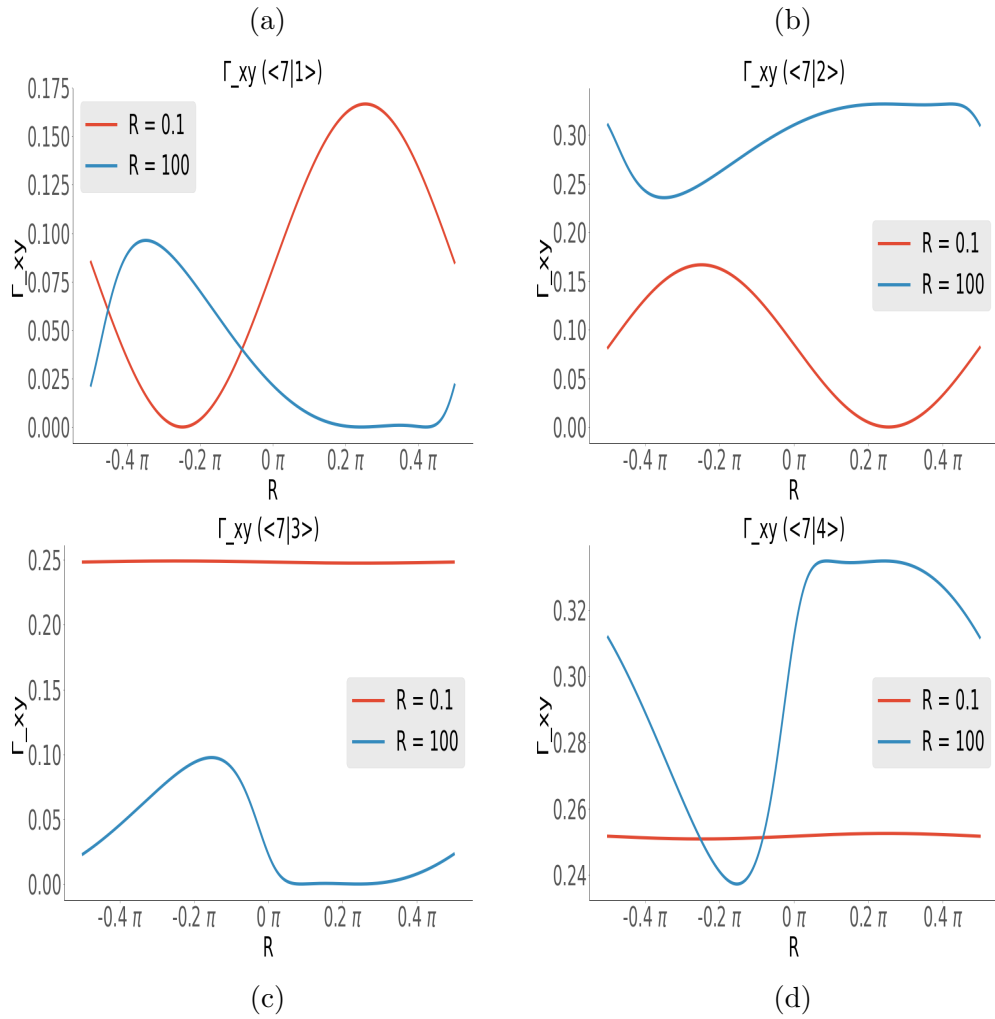


Figure 4.9: Plot of function  $\Gamma_{xy}$  vs theta in the overall regime. Figure (a) corresponds to Fig4.2 (c) and Fig4.4 (a); (b) corresponds to Fig4.2 (d) and Fig4.4 (b); (c) corresponds to Fig4.2 (a) and Fig4.4 (c); (d) corresponds to Fig4.2 (b) and Fig4.4 (d)

# Chapter 5

## Conclusion and Outlook

So far, we have shown a simple model of a quantum dot with the strain effect of the band splitting and the strain anisotropy. And we calculated matrix element of electric dipole transitions. Then selection rules among these transitions have been found. Compared with the Hydrogen atom, transitions in quantum dot usually have lower transition rate, and polarization of the photon are much insensitive to the magnetic field. Looking at the results in overall regime, it is also has been shown a huge difference of selection rules between the two regimes of the ratio  $R$ . Compared them with experiment result in [1], result in the regime of small  $R$  is more close. However, this model is still very naive compared to a 'natural' QD, as we omitted some effects for the sake of calculation convenience, for example the magnetic dipole transition. Also, the electronic states, which in terms of the Bloch functions, of the QD could be more precise.

# Bibliography

- [1] Martin Hayhurst Appel, Alexey Tiranov, Alisa Javadi, Matthias C Löbl, Ying Wang, Sven Scholz, Andreas D Wieck, Arne Ludwig, Richard J Warburton, and Peter Lodahl. Coherent spin-photon interface with waveguide induced cycling transitions. *Physical Review Letters*, 126(1):013602, 2021.
- [2] M Bayer, G Ortner, O Stern, A Kuther, AA Gorbunov, A Forchel, Pawel Hawrylak, S Fafard, K Hinzer, TL Reinecke, et al. Fine structure of neutral and charged excitons in self-assembled in (ga) as/(al) gaas quantum dots. *Physical Review B*, 65(19):195315, 2002.
- [3] Richard Fitzpatrick. Quantum mechanics, the university of texas at austin, 2010.
- [4] David J Griffiths and Darrell F Schroeter. *Introduction to quantum mechanics*. Cambridge University Press, 2018.
- [5] Oliver Gywat, Hubert J Krenner, and Jesse Berezovsky. *Spins in optically active quantum dots: concepts and methods*. John Wiley & Sons, 2009.
- [6] AV Koudinov, IA Akimov, Yu G Kusrayev, and F Henneberger. Optical and magnetic anisotropies of the hole states in stranski-krastanov quantum dots. *Physical Review B*, 70(24):241305, 2004.
- [7] Y Léger, L Besombes, L Maingault, and H Mariette. Valence-band mixing in neutral, charged, and mn-doped self-assembled quantum dots. *Physical Review B*, 76(4):045331, 2007.
- [8] F Tinjod, B Gilles, S Moehl, K Kheng, and H Mariette. Ii–vi quantum dot formation induced by surface energy change of a strained layer. *Applied Physics Letters*, 82(24):4340–4342, 2003.